Thermodynamic Properties of AgCl - KCL - LiCl Melts

Thermodynamic Properties of Silver Chloride Potassium Chloride-Lithium Chloride Melts

by

Anthony Charlton Gruner

A thesis submitted to the Faculty of Graduate Studies and Research in Partial Fulfilment of the Requirements for the degree of Masters of Engineering.

Department of Metallurgical Engineering
McGill University

February 1974

Propriétés thermodynamiques de mélanges de chlorures d'argent, de potassium et de lithium

RESUME

Les propriétés thermodynamiques molaires partielles du chlorure d'argent liquide dans des solutions fondues de chlorure de potassium - chlorure de lithium ont été mesurées à l'aide d'une cellule du type

$$- Ag/AgCl - KCl - LiCl/Cl_2, C +$$

Le domaine de température étudié s'étend de 370 à 530°C. Un modèle qui rend compte semi-quantitativement du comportement observé a été appliqué au système ternaire.

M. Eng., Metallurgical Engineering

Anthony Charlton Gruner

Thermodynamic Properties of Silver Chloride-Potassium Chloride-Lithium Chloride Melts

ABSTRACT

Partial molar thermodynamic properties of liquid silver chloride in molten potassium chloride-lithium chloride solutions were measured using a cell of the type:

$$- Ag/AgCl - KCl - LiCl/Cl_2, C +$$

The temperature range investigated was 370 to 535°C. An ionic theory was applied which would semi-quantitatively account for the observed behaviour.

ACKNOWLEDGEMENTS

This research project was performed under the supervision of Dr. W.T. Thompson whose guidance is sincerely appreciated.

An acknowledgement is due to Professor W.M. Williams and all other members of the Department.

A special note of thanks is due to Mr. J.P. Sadocha who has done a commendable job in drawing the figures.

The author is indebted to the National Research Council of Canada for providing financial assistance.

Finally, a great tribute must be given my wife, Wendy, with whose support this work has been undertaken.

TABLE OF CONTENTS

LIST OF FIGURES

INTRODUCTION

Since the inception of electrolytic practices in the middle of the nineteenth century, they have acquired increasing importance in the extraction and refining of metals. At present electrochemical procedures are involved in the production of at least half the common nonferrous industrial metals. The most notable is the electrowinning of aluminum with a world production of approximately 10 million tons per annum.[1]

Electrolytic processes may be distinguished by the nature of the electrolytes employed; aqueous or fused salt. Aqueous electrolytes are appropriate only for relatively noble metals where the discharge of hydrogen ions cannot compete for thermodynamic or kinetic reasons with the discharge of metallic ions. For more reactive metals the discharge of hydrogen ions virtually prevents the deposition of the metal. For these metals fused halide electrolytes are generally employed. Fused electrolytes are particularly appropriate since they have high electrical conductivity and permit electrolysis to be conducted at high current density - one order of magnitude greater than that usually obtained with aqueous electrolytes. These advantages considerably outweigh the expenditure of energy required to maintain the electrolyte in the molten state.

At the present time, the only metals electrowon on a large scale from fused electrolytes have melting points lower than that of the electrolyte. These include sodium, magnesium and aluminum. Since they are consequently reduced in the liquid state there are no difficulties associated

with cathode morphology or separation of the reduced metal from the electrolyte.

Much research has shown that it is possible in principle to deposit high melting point metals such as titanium and zirconium from fused salts. The idea is attractive since it would make these potentially abundant metals available at low cost. However, deposits of these metals, almost without exception, are dendritic in nature especially when the electrolyte does not contain fluoride. As a result there is considerable practical difficulty in operating the cell continuously and separating the deposit from the electrolyte. In addition, expensive melting of the deposit is required in order to produce it in a form suitable for subsequent processing.

In recent years there has been an effort directed towards elucidating the mechanism of dendrite development during deposition from fused electrolytes.[26] All such theories ultimately require knowledge of the properties of molten electrolytes and in particular "ionic structure". Consequently, numerous fundamental studies of molten salts and mixtures thereof have been conducted by metallurgists in the past two or three decades. Of basic importance is a knowledge of the thermodynamic properties of salt solutions which relate to melt structure. These are prerequisite to any theories concerned with electrode kinetic phenomena of which dendritic growth is but one.

Thermodynamic studies have generally been restricted to binary systems in spite of the importance of ternary solutions in many practical electrolyte systems. In recent years, however, there has been a systematic

investigation of the comparatively easy to study silver chloride alkali chloride ternary systems; these include the systems silver chloride - sodium chloride - potassium chloride and silver chloride - sodium chloride - cesium chloride[2] and most recently, silver chloride - sodium chloride - rubidium chloride.[3] These systems are particularly suited to accurate study since they are relatively non-hygroscopic, have low vapour pressure and can be studied by established electrochemical means. The properties of all these systems are much the same because of the chemical similarity of the alkali metals from sodium to cesium. It is expected that there would be much different behaviour for a ternary system of silver chloride containing lithium chloride because of the small ionic radius of lithium. Consequently, a study of this melt could contribute significantly to the general understanding of molten salt solutions.

This report is concerned with the study of the thermodynamic properties of the molten silver chloride - lithium chloride - potassium chloride system. This system is somewhat more difficult to study than those cited previously because of the tendency of lithium chloride to react with atmospheric water vapour to form lithium hydroxide and hydrochloric acid vapour. For this reason precautions were required in handling and preparing the melt - practices which as previously indicated are not necessary when dealing with the other alkali chloride melts. However, in other respects this system is amenable to precise study especially because of the low temperature eutectic in the lithium chloride - potassium chloride binary. This permits useful data to be gathered on the melt without the necessity of measurements at temperatures in excess of 535°C.

EXPERIMENTAL PROCEDURE

Thermodynamic properties of molten silver chloride - lithium chloride - potassium chloride electrolytes were determined by measuring the Gibbs free energy change for the reaction

$$Ag_{(s)} + \tfrac{1}{2}Cl_{2(g)} \rightarrow AgCl_{(l)}$$

in electrolytes of different silver chloride concentrations over the approximate temperature range of 370 to 535°C. The electrochemical cell

$$- Ag \;/\; AgCl - LiCl - KCl \;/\; Cl_2, C +$$

was employed exclusively in this work.

The technique was suitable since the chlorine electrode is known to be reversible and, as a result, voltage measurements are stable and reproducible; moreover, such cells have been successfully used in several prior investigations on similar systems.[3,4]

Salt Purification

Although reagent grade salts* were employed for all electrolytes some purification was required since lithium chloride reacts with water.

$$H_2O + LiCl \rightarrow LiOH + HCl$$

Besides directly contaminating the melt, the hydroxide is undesirable because it reacts with the pyrex containers used throughout the experiment.

---

* Refer to Appendix B for a complete listing of the sources of materials.

The electrolyte was purified by a method developed by Laitinen, Ferguson and Osteryoung.[5] This principally involves passing anhydrous HCl vapour over the lithium chloride to shift the above reaction to the left.

The purification of the salt took place in the apparatus shown in Figure 1. This apparatus was constructed from pyrex glass and consisted of two major parts which were connected by means of an O-ring joint and clamp. This type of design facilitated the removal of the upper part so that access to the melt or a change of the upper portion of the apparatus could be carried out quickly.

The lower portion of the apparatus consisted of a large outer tube 54 cm long and 50 mm. in diameter. At the open end of this tube the O ring ball joint 50 mm. ID. was attached. This large tube had pyrex wool at the bottom, on top of which sat the pyrex crucible which held the melt. This part of the apparatus was held by a clamp over a central tube furnace which was on a track. This enabled the top of the furnace to be moved to any position along the outer tube up to the ball joint assembly.

The upper portion of the apparatus consisted of a head containing three openings and an inner tube slightly smaller in diameter than the head, approximately 40 cm. long which ended in a tapered opening 12 mm. in diameter.

The largest of the three openings was located in the center of the head and consisted of a male ground glass joint. The female portion of this joint contained an O-ring seal which in turn accommodated a lance. An advantage of this type of seal was that it allowed the pyrex lance to

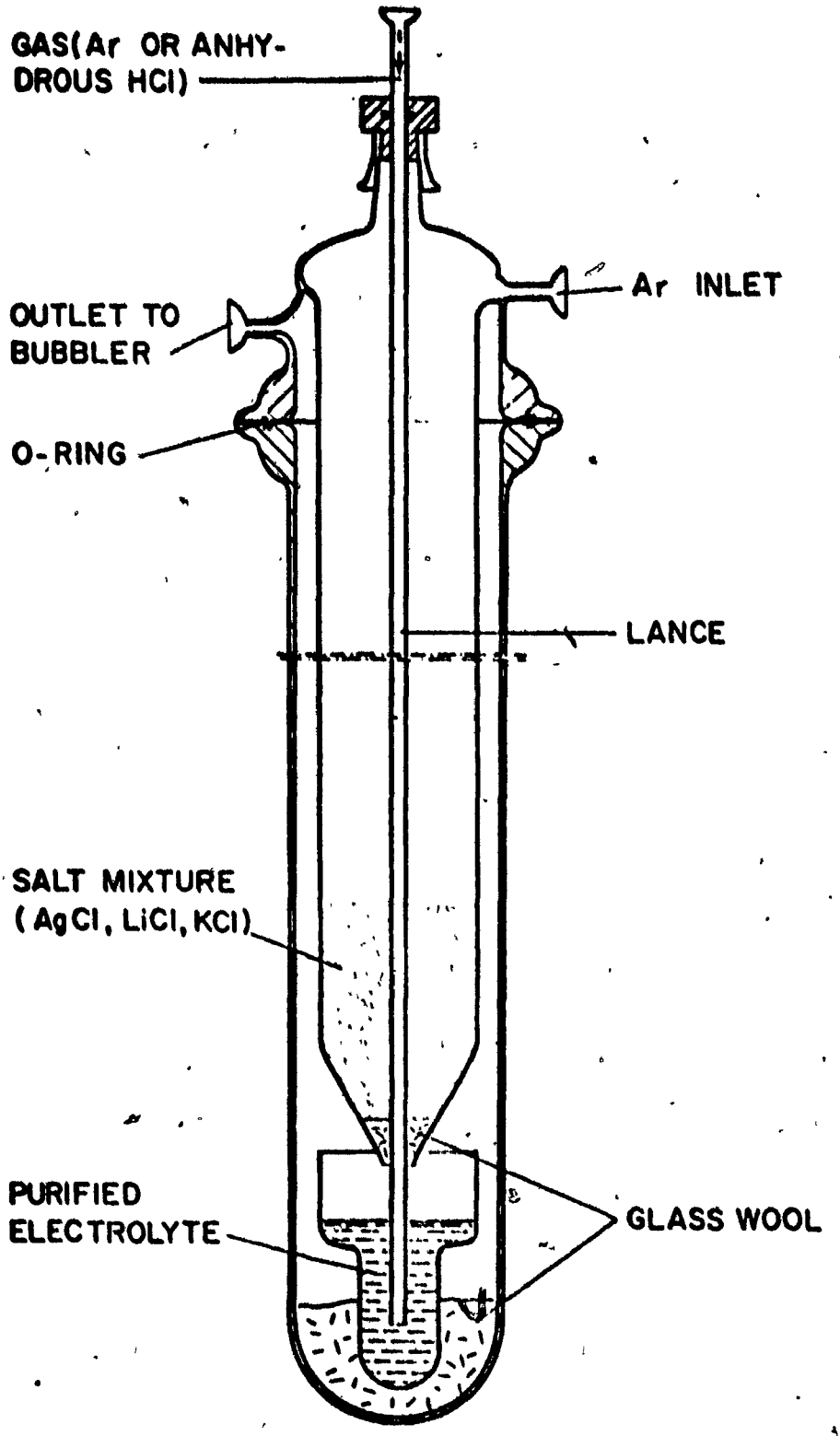

FIGURE 1. Salt purification cell.

have its position altered without any gas escaping through the seal or, conversely, preventing gas from leaking into a vacuum. The other two openings used for gas line connection had the ball and socket type joints. One of these openings gave access to the inner tube; the other led from the space between the head and the inner tube.

The salt mixture was purified in the following manner. Glass wool was packed just above the taper of the inner tube. The lance was passed through the pyrex wool and out through the taper. The salt mixture was introduced to the chamber through the large central opening and rested on the pyrex wool. The ground glass joint was closed and the appropriate gas line connections were made to the ball joints.

The assembly was then evacuated for a period of two hours at room temperature; the temperature was increased, over a period of five hours, to 300°C. During this time the vacuum was maintained at .03 Torr.

At 300°C the apparatus was filled with argon, dried by passing over magnesium perchlorate, and made virtually oxygen free by reaction with copper at 500°C. Refer to Figure 2. When the pressure in the apparatus was slightly greater than atmospheric, the argon was shut off and anhydrous hydrogen chloride was passed through the salt mixture before being exhausted to the exit bubbler.

The temperature of the furnace was raised to 500°C while the anhydrous hydrogen chloride gas passed through the salt mixture. In the temperature range 352°C and 400°C, the salts fused and trickled through the pyrex wool filter into the crucible. Insoluble matter present in the

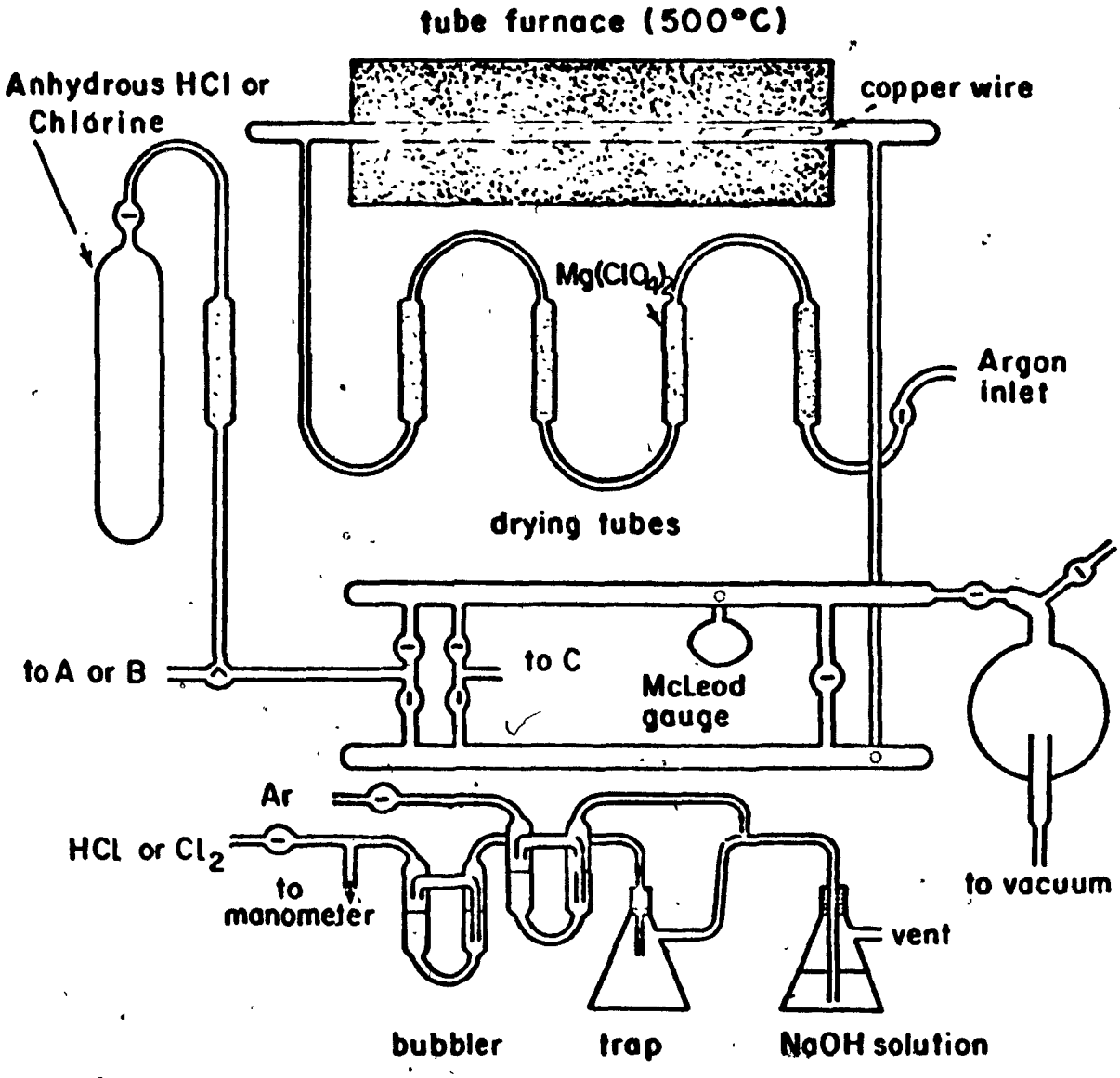

A– chlorine electrode
B– salt purification cell
C– cell inlet for argon

FIGURE 2. Schematic diagram of argon purification train and auxiliary equipment.

salt mixture was not melted and was retained by the pyrex wool. When fusion of the salt mixture was complete the lance was lowered into the molten salt solution and anhydrous hydrogen chloride gas was bubbled through the melt. To purge the system of hydrogen chloride gas, argon was bubbled through the melt for two hours.

Electrochemical Cell

The electrochemical cell which is shown in Figure 3 was assembled by removing the salt purification chamber from the large pyrex tube containing the crucible with the purified salt solution, and immediately replacing it with a cell cover containing five orifices. This pyrex cell cover was clamped to the O-ring ball joint; the gas lines were connected and the argon flow was established in order to purge the atmosphere over the salts of any air that had entered the apparatus during the change over.

Of the five openings in the cell cover two were required for inlet and outlet of the argon flow. A third opening provided entry for the thermocouple well. Silver and chlorine electrodes were installed through the remaining two openings.

The opening for the thermocouple well contained the O-ring seal, which allowed the thermocouple to be raised or lowered in the melt. This was advantageous in that the position of the couple within the melt could be adjusted. A chromel-alumel thermocouple calibrated against the melting points of lead and antimony was employed for all temperature measurements.

The silver electrode was a pure silver wire 3 mm. in diameter and was immersed approximately 2.5 cm. into the melt. The silver electrode

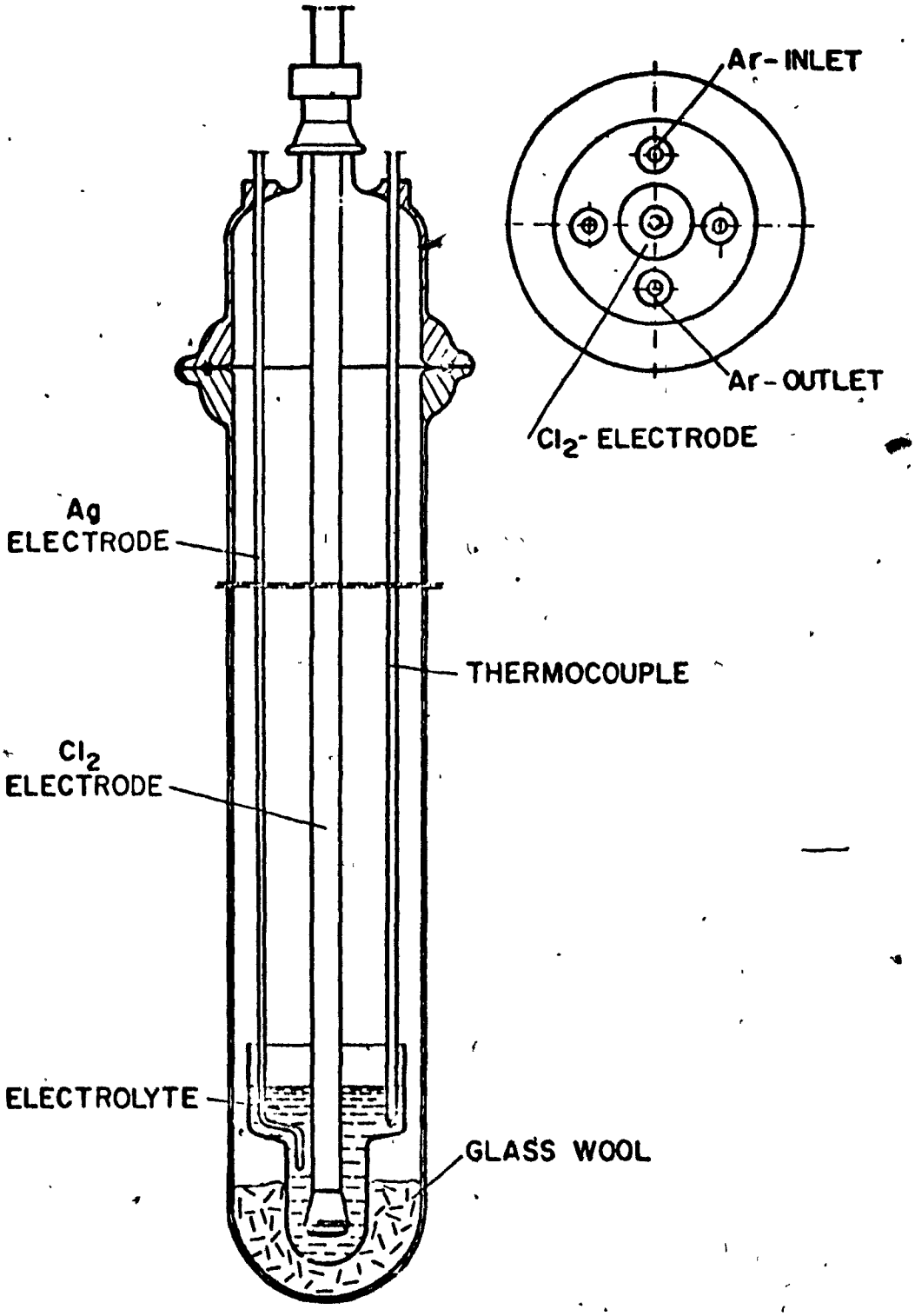

FIGURE 3. Electromotive force cell.

entered the inside of the apparatus through an O-ring seal.

Chlorine Electrode

At the center of the cell cover was the male portion of a ground glass joint the same size as the one used for the salt preparation chamber. Through this opening was placed the chlorine electrode fitted to an O-ring seal. The chlorine electrode basically consisted of a graphite rod in contact with the electrolyte and a chlorine atmosphere. A detailed drawing appears in Figure 4.

The graphite electrodes were 6 mm. in diameter and were special spectroscopic grade "SPK" graphite from the National Carbon Company. The graphite rods were pre-treated by chlorination. Briefly, the method consists of holding the graphite rods at 900°C, under vacuum for 12 hours, and then under an atmosphere of chlorine for a total of forty-eight hours.

The pretreated graphite rod was placed inside a pyrex tube which was closed at the bottom end with the male portion of a ground glass joint. The pyrex tube had a few holes located about 35 mm. above the ground glass joint. At the top end, the graphite rod was connected to a brass plug which had its inner surface coated with wax to prevent a reaction with chlorine. This sealed it at the top portion of the tube; it also provided a contact point for the potentiometer leads to the graphite. Approximately an inch from the top end of the pyrex tube a ball joint was joined.

This pyrex tube was placed inside a larger pyrex tube which contained at the bottom end, the female portion of the ground glass joint. At the top side of the outer pyrex tube another small ball joint was affixed.

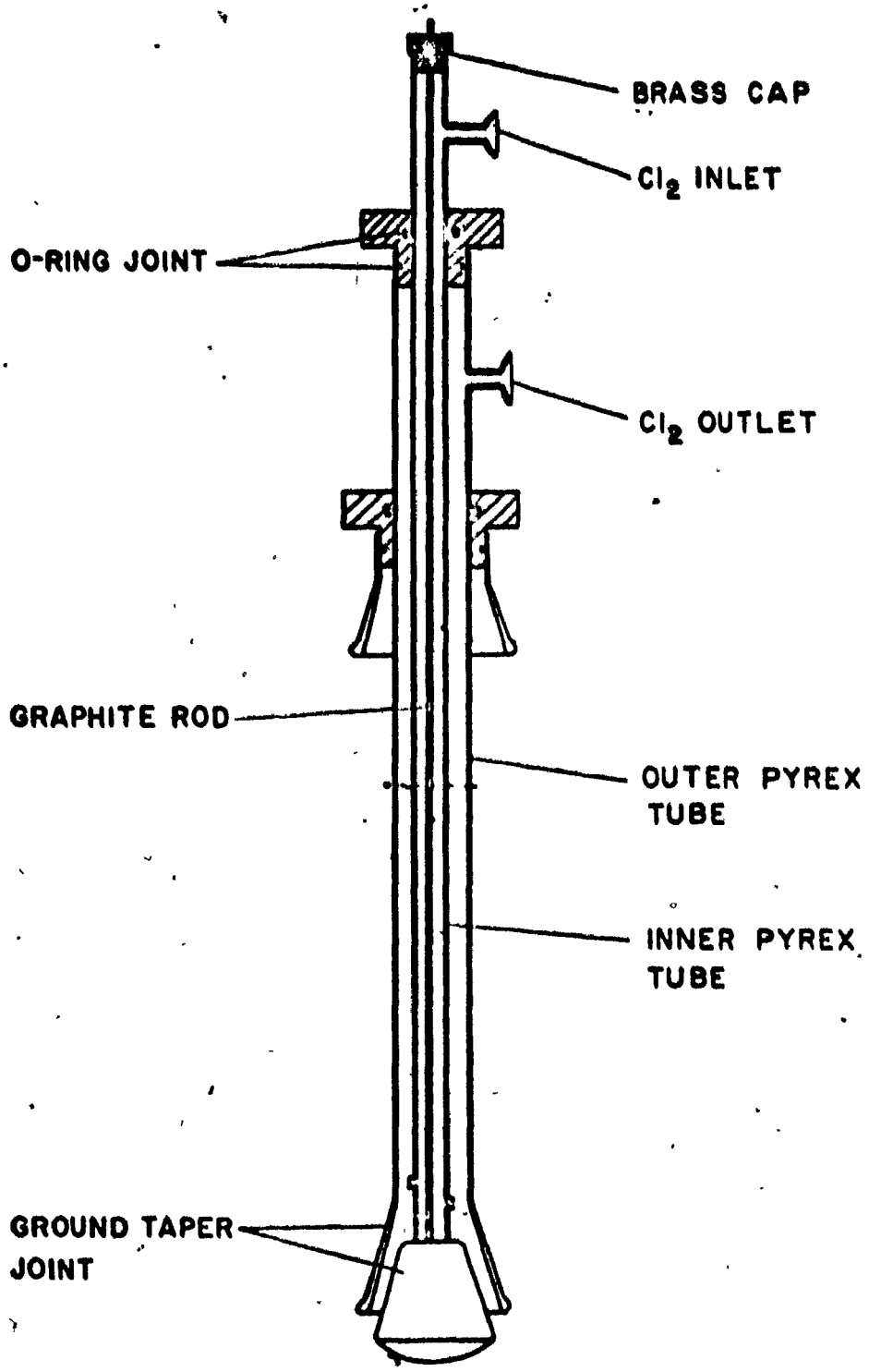

FIGURE 4. Schematic diagram of chlorine electrode.

The inner pyrex tube was capable of moving inside the outer pyrex tube; an O-ring seal joined the outer tube to the inner tube at the top end and the ground glass joint connected the tubes together at the bottom end.

When the chlorine electrode was in position, it was made operational by the following procedure. The chlorine inlet line was connected by the ball joint to the inner pyrex tube. The chlorine exhaust tube was connected to the ball joint on the outer pyrex tube of the chlorine electrode. Argon was then introduced into the line to flush the air from the electrode. The electrode was then lowered into the melt and the argon flow stopped. The inner tube was pushed downward thus opening the tapered joint. The molten electrolyte flowed into the inner tube and around the graphite electrode. The outer tube of the electrode was pushed down to close the ground glass joint and trap a small amount of molten salt in contact with the graphite electrode.

The resistance the ground glass joint created in the cell when closed was between 500 and 3000 ohms, as measured with a conductivity bridge. The importance of creating as high a resistance as possible is to reduce the chlorine diffusion from the electrode. If chlorine diffused into the melt it would react with the silver electrode thus increasing the concentration of silver chloride in the melt which would decrease the electromotive force between the silver and chlorine electrode.

Dried chlorine gas was introduced to the inner tube containing the graphite rod and flowed downwards over the trapped melt and passed through the small holes above the melt into the outer tube. It then flowed upwards and was exhausted from the electrode.

Typical Experiment

The electromotive force measurements were conducted on pure silver chloride and 13 ternaries. The e.m.f. measurements of the ternary mixtures were made along lines of constant ratio of potassium and lithium chloride while the concentration of silver chloride was increased.

The silver chloride was added to the melt directly and anhydrous hydrogen chloride gas was bubbled through the melt for 15 minutes. Dried argon gas was then passed through the melt to purge it of the excess hydrogen chloride. This procedure was carried out after each addition of silver chloride to the melt.

When the e.m.f. measurements of a ternary composition were completed, two samples of the melt were taken for silver chloride and potassium chloride analysis.

The analysis was carried out by dissolving the frozen salt mixture in ammonium hydroxide and distilled water. The silver chloride was precipitated from the solution after expelling the ammonium hydroxide.[6] The precipitate was collected by filtering, then drying and weighing to a constant weight to give the percentage by weight of silver chloride.

The filtrate was saved and then analysed, for potassium by using the perchlorate method[7], where the potassium is precipitated in the form of potassium perchlorate by reacting it with perchloric acid. The lithium perchlorate which also forms is dissolved preferentially in an organic solvent. The potassium perchlorate is collected by filtering, dried and weighed, to determine the percentage potassium chloride.

The lithium chloride was determined by the difference of potassium chloride and silver chloride from the total sample weighed.

During sampling partial freezing of the electrolyte may occur resulting in some sample bias due to segregation. This and other systematic errors accumulate so that the composition reported should be regarded as not more accurate than one mole percent.

The e.m.f. readings were made in the temperature range between 370 and 535°C, the upper limit being the temperature at which the pyrex begins to soften. The lower limit is dictated by the freezing point of the salt. The e.m.f. measurements were made on increasing then decreasing the temperature to predetermined values.

The chlorine gas took about 12 hours to saturate the melt and achieve equilibrium. Once saturated it responded immediately to changes in the chlorine pressure. The chlorine pressure was measured with a manometer and typically was about 10-12 torr above the atmospheric pressure because of the exit bubbler head.

Voltage was stable to within 0.2 mv for a period of one hour. The cell responded immediately to changes in temperature. The cell e.m.f. was measured with Leeds and Northrup K-4 potentiometer and standardized against an Eppley cell.

The temperature gradient within the melt was determined to be about 0.4 C^{o} cm^{-1}. Since the overall depth of the melt was approximately 10 cm., the total absolute error in temperature measurements is about $\pm$ 2 C^{o}.

EXPERIMENTAL RESULTS AND DATA ANALYSIS

For the electrochemical cell:

$$- Ag/AgCl/Cl_2, C +$$

the primary cell process is

$$Ag_{(s)} + \tfrac{1}{2} Cl_{2(g)} \rightarrow AgCl_{(l)} \qquad (1)$$

for which the Nernst expression is

$$E = E^o - \frac{RT}{F} \ln \frac{a_{AgCl}}{p_{Cl_2}^{\frac{1}{2}}} \qquad (2)$$

where the standard states are pure solid, gas at 1 atmosphere pressure, and pure liquid for silver, chlorine and silver chloride respectively. Refer to Appendix A for nomenclature.

The measured e.m.f. does not give E directly because of the thermoelectric effect associated with dissimilar electrodes. The silver and carbon electrodes effectively constitute a thermocouple in-series with the electrochemical cell. A correction for this effect can be made by applying the equation

$$E(mv) = 4.36 - .08802T + .01288T \ln T \qquad (3)$$

which relates the thermoelectric voltage to the temperature of the hot junction, (the melt temperature), when the cold junction, (the external terminal temperature), is 25°C. Since this potential has the opposite polarity to that of the electrochemical cell the correction is added to the measured e.m.f.[3].

Rearranging equation (2)

$$E - \frac{RT}{2F} \ln P_{Cl_2} = E^o - \frac{RT}{F} \ln a_{AgCl} \quad (4)$$

$$E^* = E - \frac{RT}{2F} \ln P_{Cl_2} \quad (5)$$

E^* is the potential of the cell with respect to the standard chlorine electrode, that is to say one in which the chlorine pressure is 1 standard atmosphere.

All experimental e.m.f.'s are tabulated in Appendix C. E^* is also listed.

Formation Potential of Pure Silver Chloride

In order to determine the thermodynamic properties associated with the mixing of AgCl in molten LiCl and KCl, the standard formation potential of pure AgCl must be known as a function of temperature. When pure silver chloride is used the activity of silver chloride is 1 in which case E^* is E^o.

Although several investigations have reported values for E^o (8,9,10,11,12,13,14), a redetermination was undertaken in order to test the operation of the cell. These measurements are depicted in Figure 5 .

In order to achieve a satisfactory interpolation of the measurements, a regression analysis was performed recognizing the known difference in the heat capacity between silver chloride, silver and chlorine gas.

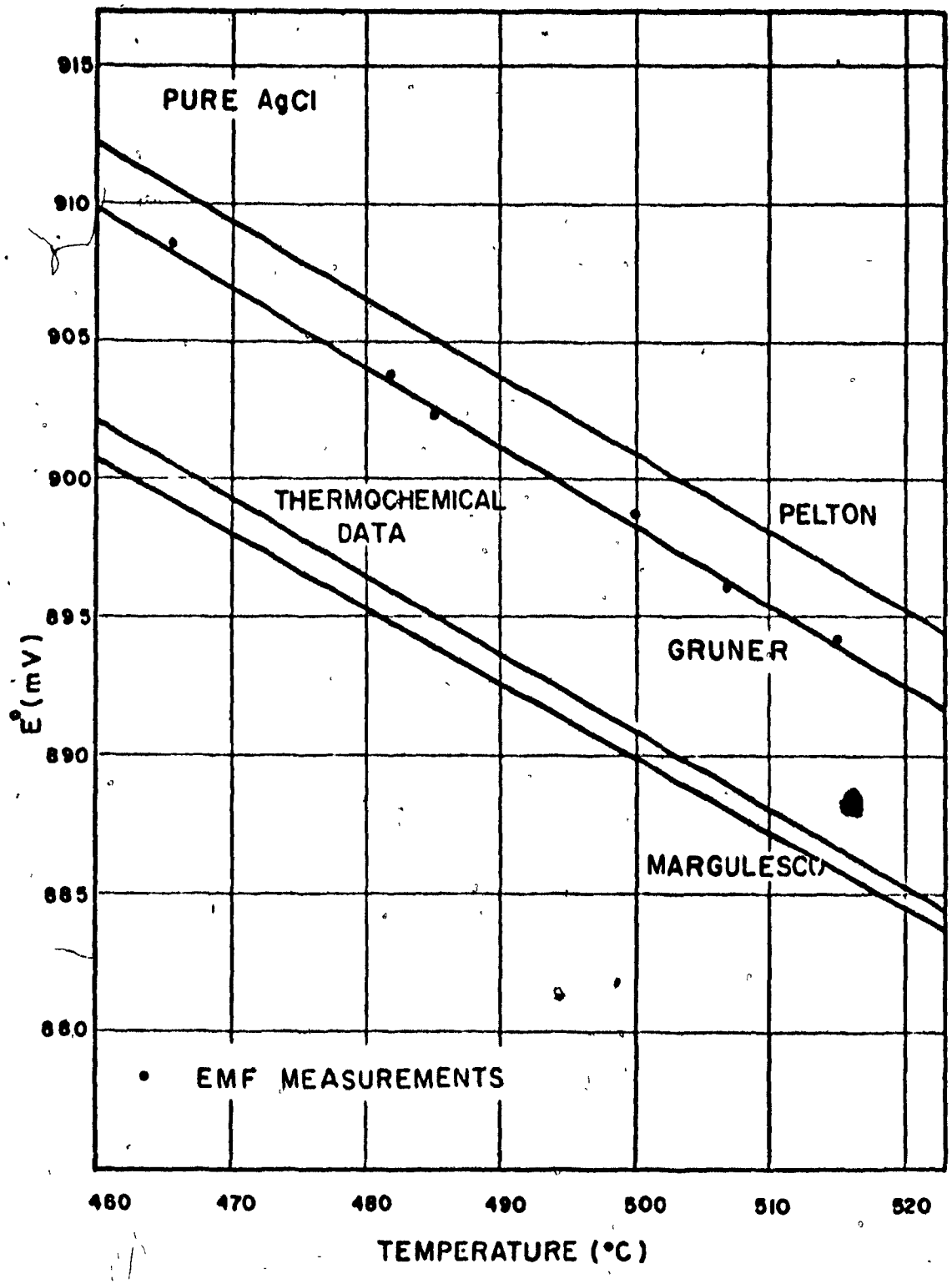

FIGURE 5. e.m.f. vs. temperature curve for pure AgCl

This difference causes a slight but significant curvature in the E^o versus T line which is important in extrapolating the measurements to a higher or lower temperature. Using the tabulated values from Kubaschewski[15] for silver and chlorine and the measurements of Thompson and Flengas[16] for liquid silver chloride

$$(\Delta Cp)_1 = (Cp)_{AgCl_{(l)}} - (Cp)_{Ag_{(s)}} - \tfrac{1}{2}(Cp)_{Cl_{2_{(g)}}} \qquad (6)$$

$$= + 4.195 - 2.07 \times 10^{-3}T - .02 \times 10^{5}\, T^{-2}$$

$$\text{cal. g. mole}^{-1}\ K^{-1}$$

It follows that

$$\Delta H^o = \Delta H_o^o + 4.195T - 1.035 \times 10^{-3}T^2 + .02 \times 10^{5}T^{-1} \qquad (7)$$

$$\Delta S^o = \Delta S_o^o + 4.195\ \ln T - 2.07 \times 10^{-3}T + .01 \times 10^{5}T^{-2} \qquad (8)$$

where ΔH_o^o and ΔS_o^o are integration constants.

Since $\Delta G_T^o = - FE^o$ (9)

and $- FE^o = \Delta H^o - T\Delta S^o$ (10)

it follows that

$$- FE^o - 4.195T + 4.195T\ \ln T - 0.01 \times 10^{5}T^{-1}$$

$$-1.035 \times 10^{3}T^2 = I \qquad (11)$$

where

$$I = \Delta H_o^o - T\Delta S_o^o \qquad (12)$$

a linear regression of ξ versus T gives values of -28449 cal. g. mole^{-1} for ΔH_o^o and -32.899 cal. g. mole^{-1} K^{-1} for ΔS_o^o. The standard deviation for this regression analysis was .082.

The variation of E^o with respect to temperature is displayed in Figure 5.

The highest reported measurements[8] and lowest reported measurement[12] bracket the present work. A fourth line indicating the expected variation based upon calculation from independent thermochemical data also is shown. This calculation involves an independent evaluation of the integration constants in equations (7,8).

$$\Delta H_o^o = \Delta H_{298}^o + \int_{298}^{727} (\Delta Cp)_2 \, dT + (\Delta H_{(f)})_{AgCl}$$

$$+ \int_{727}^{0} (\Delta Cp)_1 \, dT = -28199 \qquad (13)$$

$$\Delta S_o^o = \Delta S_{298}^o + \int_{298}^{727} \frac{(\Delta Cp)_2}{T} \, dt + (\Delta S_{(f)})_{AgCl}$$

$$+ \int_{727}^{0} \frac{(\Delta Cp)_1}{T} \, dT = -32.33 \qquad (14)$$

where

$$(\Delta Cp)_2 = (Cp)_{AgCl_{(s)}} - (Cp)_{Ag_{(s)}} - \tfrac{1}{2}(Cp)_{Cl_{2(g)}} \qquad (15)$$

$$= .370 + 5.87 \times 10^{-3} T - .02 \times 10^{5} T^{-2}$$

and the subscript (f) indicates fusion.

In conclusion, within a few mv ($\pm$ 6) the various determinations of E^o concur; for all subsequent calculations the following equation based upon the Σ function calculation on the present measurements will be employed.

$$E^o = 1233.6 - 1.609T + .182T \ln T - 43.36T^{-1} - 4.48 \times 10^{-5}T^2 \quad (16)$$

Relative Partial Molar Properties

A total of thirteen different compositions in the silver chloride lithium chloride, potassium chloride ternary system were studied. The compositions are depicted on the Gibbs triangle shown in Figure 6. Points on the silver chloride - potassium chloride binary are those of Pelton[17]. Points on the silver chloride - lithium chloride binary are those of Panish[18]. The compositions studied in this investigation were limited to the central region of this system because of the pyrex construction of the apparatus which limited the upper temperature of this investigation to 535°C.

The e.m.f. is measured between a standard chlorine electrode and a silver electrode and these measurements are plotted versus temperature. The resulting graphs are shown in Figures 7,8.

The general scatter of points is comparable with that of Panish et al. and Pelton shown in Figures 9 and 10 respectively. In this respect it should be pointed out that the voltage and temperature scales are more expanded for the present measurements owing to the limited temperature range. The lines in Figures 7,8,9,and10 represent traces of a regression analysis performed on all the data at once. The details and implications of the regression analysis follow.

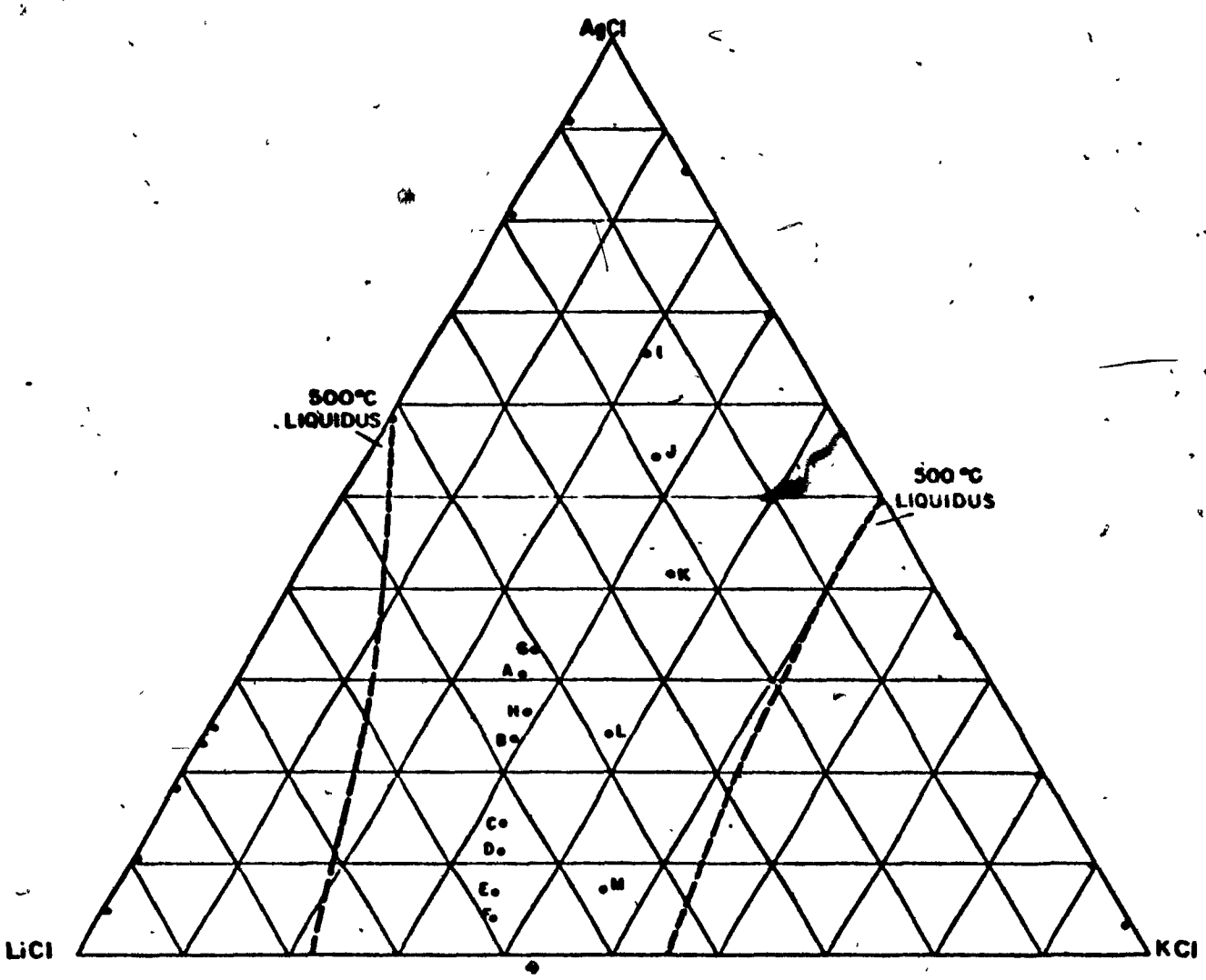

All ternary compositions are subsequently referred to by the letter code system used in this presentation.

FIGURE 6. Compositional points on ternary diagram used in this work.

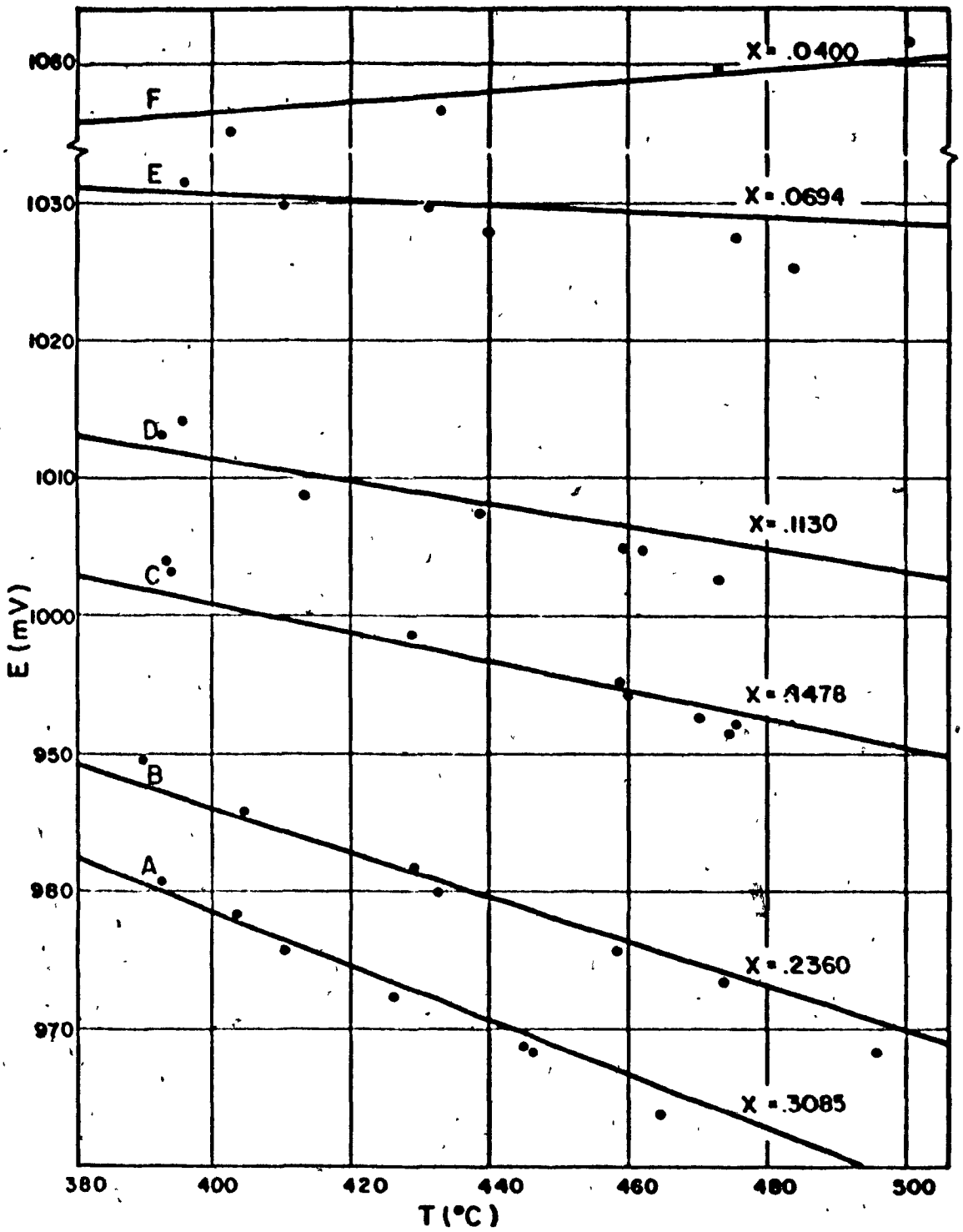

FIGURE 7. e.m.f. vs. temperature of AgCl in the AgCl-LiCl-KCl system at compositions A,B,C,D,E,F.

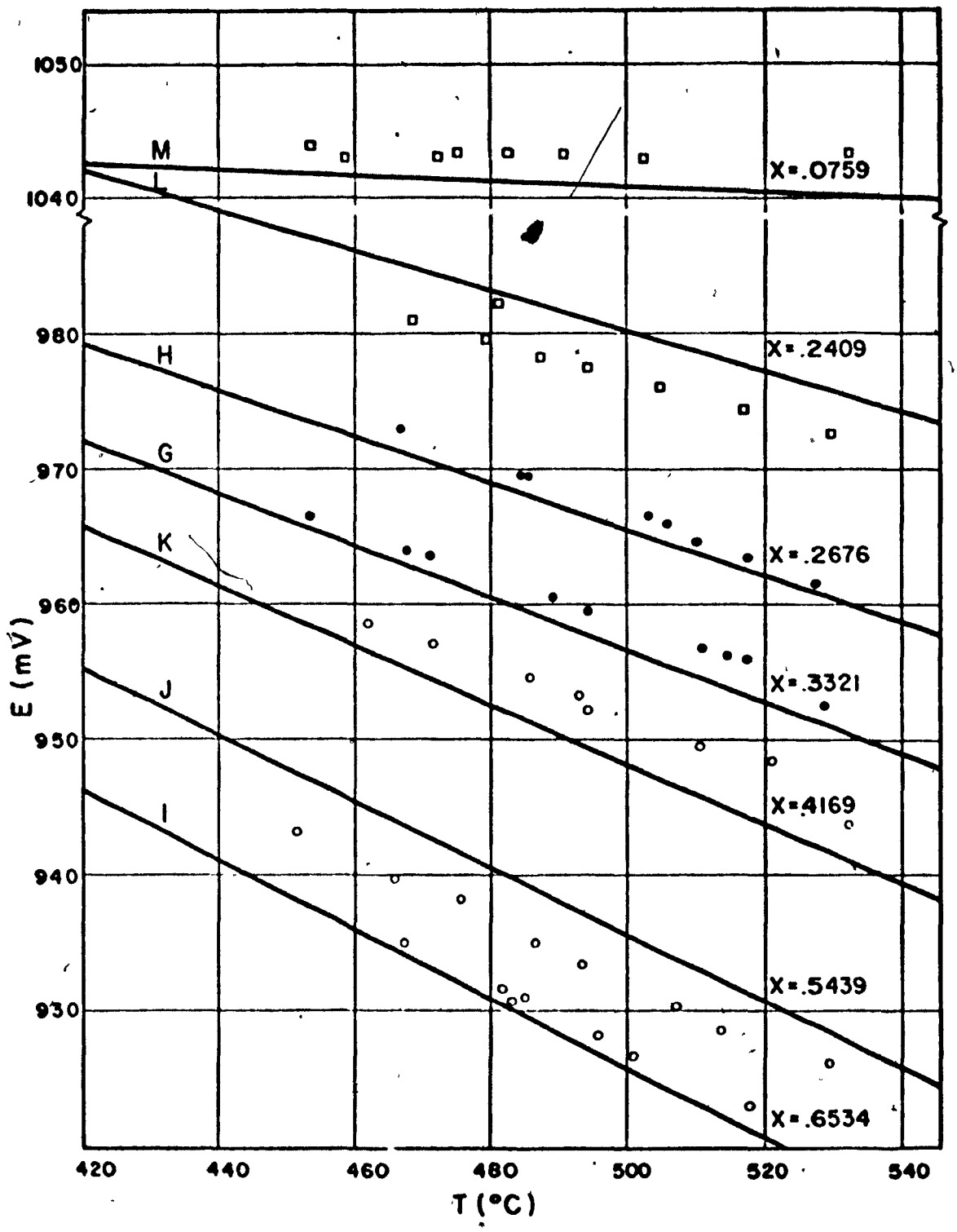

FIGURE 8. e.m.f. vs. temperature of AgCl in the AgCl-LiCl-KCl system at compositions G,H,I,J,K,L,M.

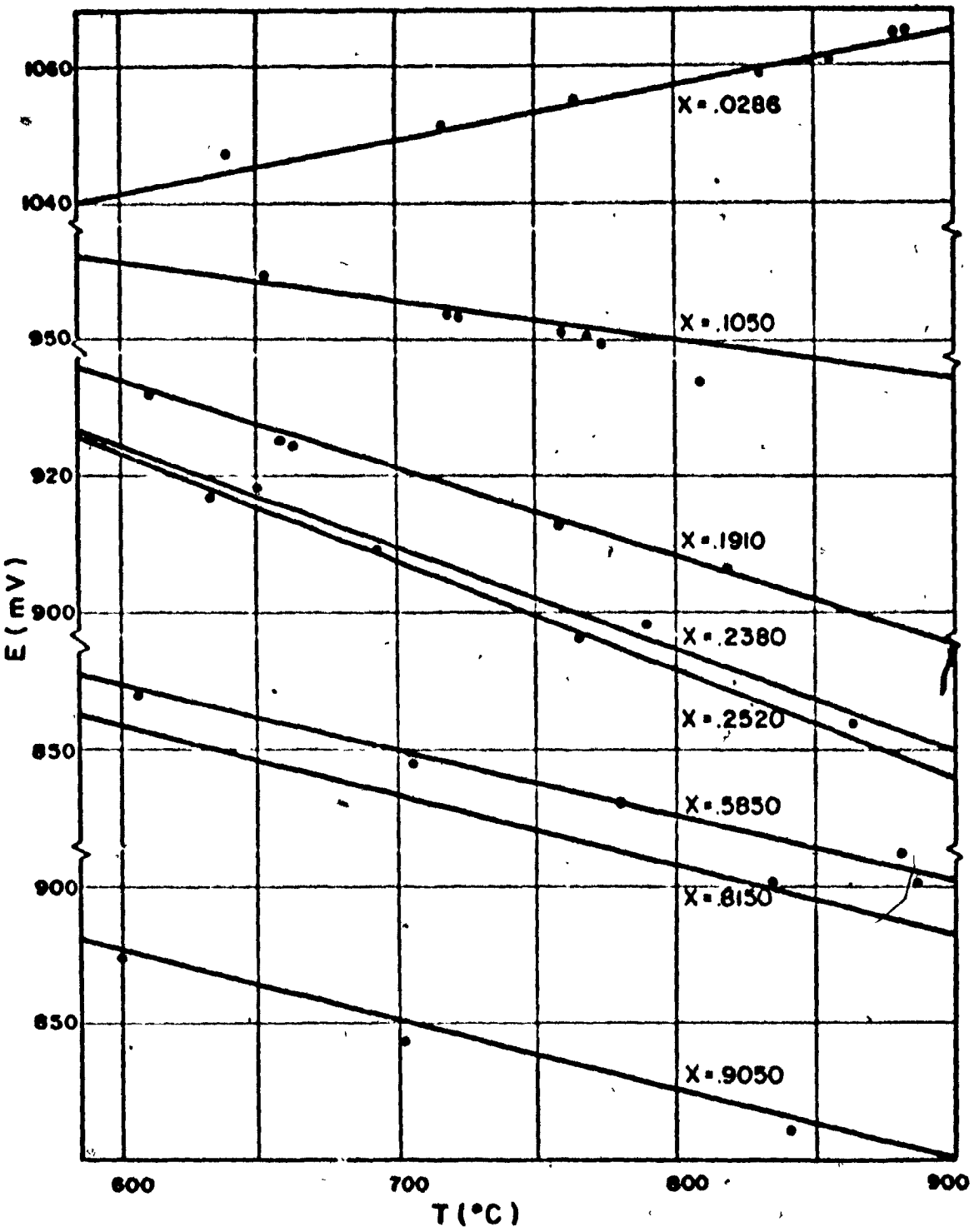

FIGURE 9. e.m.f. vs. temperature in the AgCl-LiCl system from Panish.

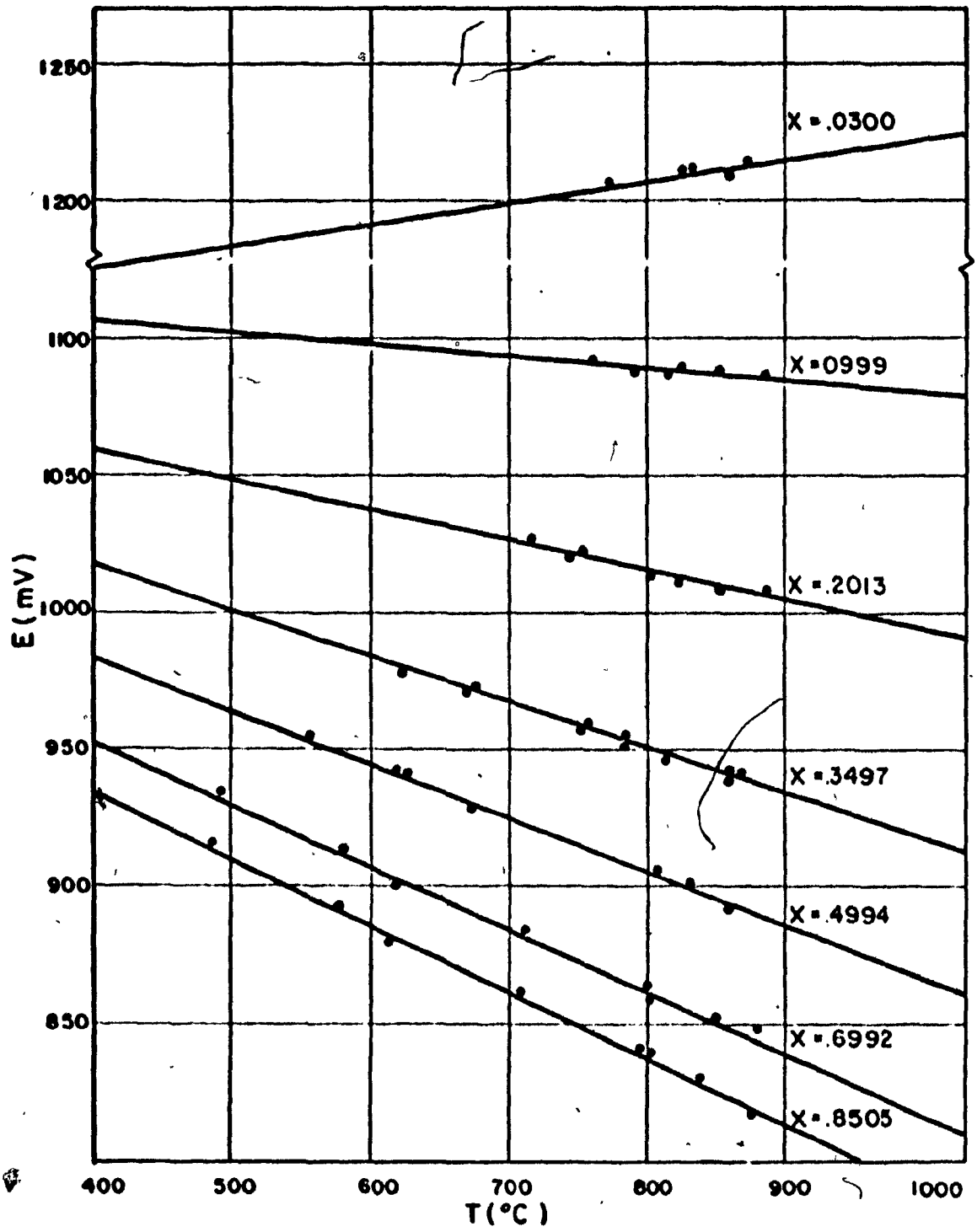

FIGURE 10. e.m.f. vs. temperature in the AgCl-KCl system from Pelton.

Regression Analysis

The difference between the electromotive force of a cell in which silver chloride is dissolved in lithium chloride and potassium chloride melt, E^*, and that of a cell involving pure silver chloride, E^o, gives the free energy of mixing for the following process.

$$1(AgCl)_{(1)} + n((Ag, Li, K)Cl)_{(1)} \rightarrow (n+1)((Ag, Li, K)Cl)_{(1)}$$

where $n >> 1$

That is to say, the relative partial molar free energy of silver chloride is

$$(\Delta\bar{G})_{AgCl} = -F(E^*-E^o) \qquad (17)$$

The relative partial molar free energy is dependent upon both the temperature and composition but is virtually unaffected by pressure changes of a few atmospheres. At fixed composition,

$$\Delta\bar{F}_{AgCl} = \Delta\bar{H}_{AgCl} - T\Delta\bar{S}_{AgCl} \qquad (18)$$

where $\Delta\bar{H}_{AgCl}$ and $\Delta\bar{S}_{AgCl}$ may be regarded as being virtually independent of temperature over an interval of a few hundred degrees.

The partial molar enthalpy and entropy, $\Delta\bar{H}_{AgCl}$ and $\Delta\bar{S}_{AgCl}$, do however vary significantly with respect to composition and the following empirical series may be employed to express this variation

$$\Delta\bar{H}_{AgCl} = \sum_{j=2} \sum_{k=o} a_{jk} (\Lambda^j)(\Psi^k) \qquad (19)$$

$$\Delta\bar{S}_{AgCl} = \sum_{j=2} \sum_{k=o} b_{jk} (\Lambda^j)(\Psi^k) - R \ln X_{AgCl} \qquad (20)$$

where $\Lambda = (1-X_{AgCl})$

and $\Psi = \dfrac{X_{KCl}}{X_{LiCl} + X_{KCl}}$

The lower limits of summation guarantee Raoultian behaviour of silver chloride in concentrated solutions. Accordingly:

$$E^* = -\frac{1}{F}\sum_{j=2}\sum_{k=0}(a_{jk} - Tb_{jk})(A^j)(Y^k)$$

$$-\frac{RT}{F}\ln X_{AgCl} + E^o \qquad (21)$$

The unknown coefficients a_{jk} and b_{jk} in the right hand side of this equation were determined by a multiple linear regression analysis based upon 198 points (103 of which were determined in this investigation the balance being obtained from Pelton[17] and Panish[18].) An arbitrary truncation of the series is required; the following twelve coefficient series was found to be adequate.

$$\begin{aligned} E^* = {} & -3895.7\,A^2 + 5.8202T\,A^2 + 3320.4\,A^2Y \\ & -7.2596T\,A^2Y - 881.3\,A^2Y^2 + .2054T\,A^2Y^2 \\ & +7114.6\,A^3 - 6.7819T\,A^3 - 3246.2\,A^3Y \\ & +4.4283T\,A^3Y - 3883.97\,A^3Y^2 + 3.5212T\,A^3Y^2 \\ & -.0862T\ln(1-A) + E^o \end{aligned} \qquad (22)$$

The standard deviation for the regression analysis is 2.47 mv; the mean absolute deviation was 1.84 mv.

As mentioned previously the lines which appear in Figures 7,8,9 and 10 represent the behaviour of equation (22) at the particular compositions involved. The notable feature is that several of the lines are systematically above or below the experimental electromotive force determinations corrected for pressure and the thermoelectric effect. This is regarded as

being due to an error associated with the determination of composition. For example, variation in the AgCl mole fraction of .01, say, from 0.40 to 0.41, consistent with the analytical accuracy discussed previously causes a change in E at 500°C of 1.6 mv. This together with probable temperature gradients in the cell are combined to account for the slight systematic deviation most apparent in Figure 8 .

Another approach to fitting the experimental measurements would have involved the independent regression of each E^* versus T and the subsequent smoothing of the enthalpy and entropy lines. However, in view of the short temperature range covered in the present study it was felt that a single data analysis in which all e.m.f.'s pertinent to this system were smoothed at once would provide a more representative empirical equation.

Equations (19),(20) & (22) make possible the evaluation of the change of $\Delta\bar{H}_{AgCl}$ and $\Delta\bar{S}_{AgCl}$ with respect to composition. The behaviour of these properties is illustrated in Figures 11 and 12 on the Gibbs triangle. Included in the plot of the relative partial entropy are dotted lines representing the ideal entropy variation as calculated using the equation

$$(\Delta\bar{S}_{AgCl})_{ideal} = - R \ln X_{AgCl} \qquad (23)$$

The behaviour of the partial excess free energy of silver chloride at 500°C is depicted in Figure 13 . This figure follows from the relative partial entropy and enthalpy calculation since:

$$\Delta\bar{G}^{E}_{AgCl} = \Delta\bar{H}_{AgCl} - T(\Delta\bar{S}_{AgCl} + R \ln X_{AgCl}) \qquad (24)$$

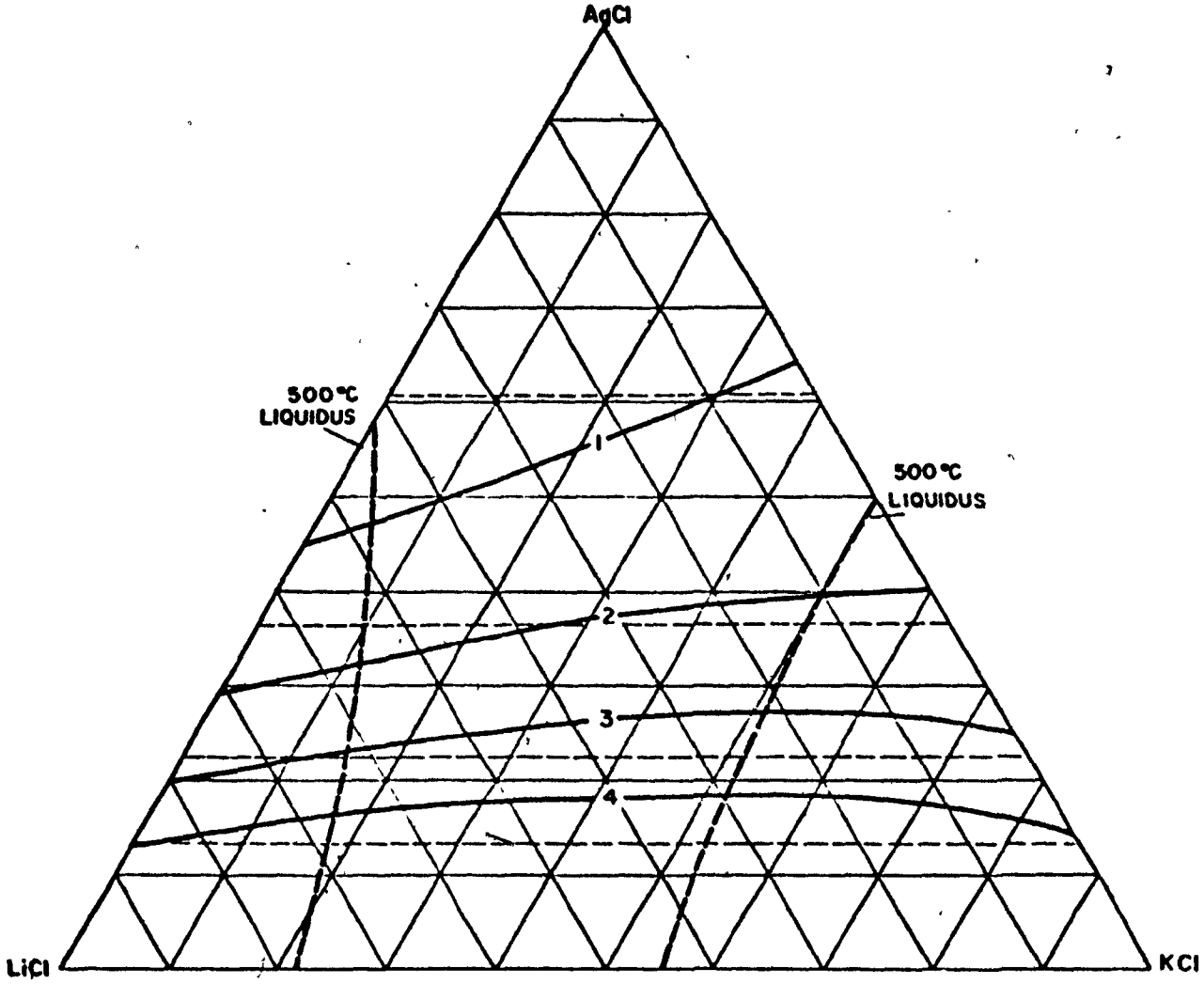

FIGURE 11. $\Delta\bar{S}$ of AgCl in the AgCl-LiCl-KCl system with $\Delta\bar{S}$ of AgCl ideal values shown as broken lines. The units are cal./°K g. mole.

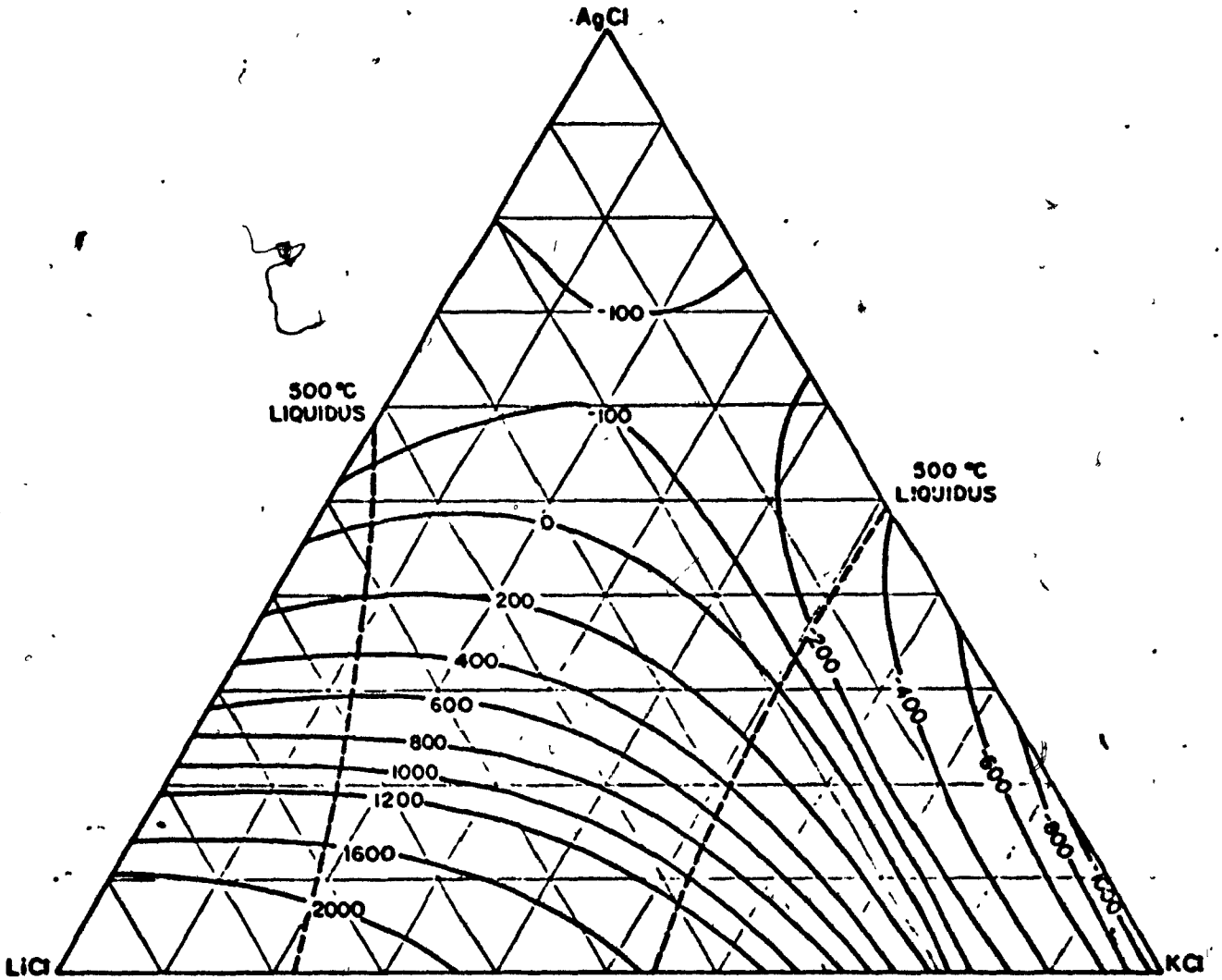

FIGURE 12. $\Delta\bar{H}$ of AgCl in the AgCl-LiCl-KCl system. The units are cal./g. mole.

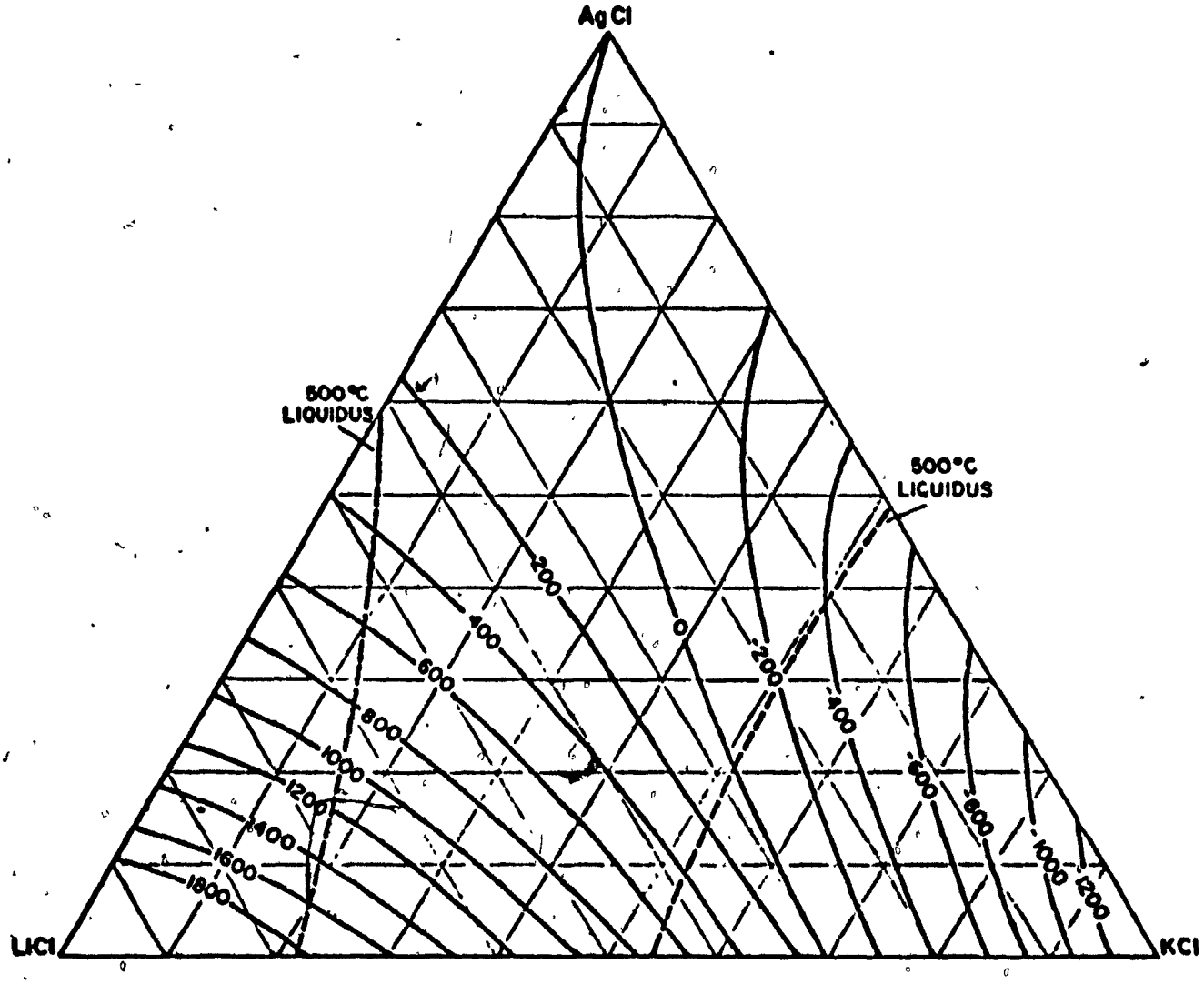

FIGURE 13. ΔG^E of AgCl at 500°C in the AgCl-LiCl-KCl system. The units are cal./g. mole.

Figure 14 illustrates the behaviour of the silver chloride activity at 500°C calculated from the excess free energy using

$$a_{AgCl} = \exp\left[\frac{\Delta \overline{G}^{E}_{AgCl}}{RT}\right] + X_{AgCl} \qquad (25)$$

All of the thermochemical calculations follow somewhat indirectly from an analysis of the entire e.m.f. measurements. This is particularly true of the entropy and enthalpy calculations which rest on an accurate knowledge of the difference in the temperature dependence of the e.m.f. of the cells containing silver chloride solutions and pure silver chloride. Accordingly, these results are not so precise as the free energy calculations based as they are on simply the differences between E^{*} and E^{o}.

DISCUSSION

In recent years there has been considerable success in interpreting the thermodynamic behaviour of molten salt solutions with ionic models that make reference to the existence of complex ions[19,20,21,22,23]. It is postulated that certain cations are more or less strongly bound to adjacent anions; these units are treated as independent entities in the melt.

Dual Bonding Model[8]

For the case of silver chloride-alkali chloride binary solutions Pelton has proposed a dual bonding model. This treatment recognizes the distinction between free silver ions and other silver ions considered to be

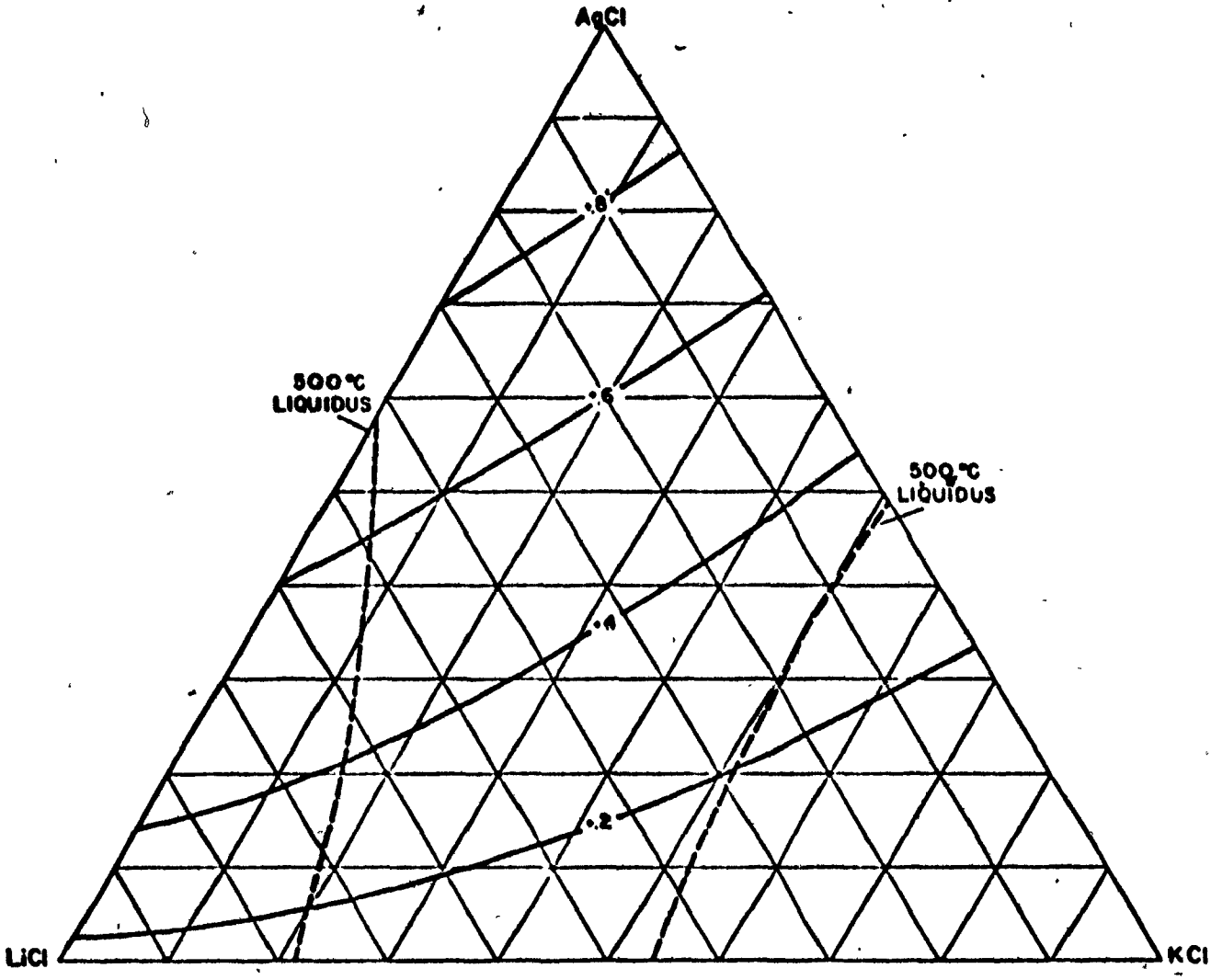

FIGURE 14. Activity isotherm for AgCl at 500°C determined experimentally.

more or less strongly bonded to adjacent anions. The model does not require postulates about the stoichiometry of this arrangement, i.e. it is immaterial whether the "bonded" silver exists as $AgCl_2^-$, $AgCl_3^=$, etc. complex ions, or, perhaps even silver chloride molecules. This treatment has had success in interpreting precisely measured thermochemical properties for the silver chloride alkali chloride binary melts- from sodium chloride through to cesium chloride. This is remarkable because of the few adjustable parameters involved in the theory - one per salt.

An extension of this treatment to the ternary melts can be made as follows. Consider the isothermal formation of a mole of molten ternary solution by combining silver chloride, and lithium and potassium chloride melt of fixed composition. This may be represented as follows:

$$X_1\ AgCl_{(l)} + (1-X_1)(Li,\ K)\ Cl_{(l)} \rightarrow (Ag,Li,K)Cl_{(l)} \qquad (26)$$

For the purpose of subsequent discussion components will be identified as follows:

AgCl - component 1
LiCl - component 2
KCl - component 3

The configurational entropy of the ternary solution is determined by the number of distinguishable ways Li^+, K^+, Ag^+, and Ag^* ("bonded" silver) can be arranged over the available cationic sites. Let this multiplicity be Ω. Regarding the number of sites for a mole of solution as simply Avogadro's number, N, and α as the fraction of the total silver that exists as Ag^* in the molten solution, the multiplicity is given by the following expression.

$$\Omega = \Omega_1 \cdot \Omega_2 \cdot \Omega_3 \tag{27}$$

where Ω_2 is the number of distinguishable ways of arranging X_2N lithium ions over N positions. Assuming random mixing

$$\Omega_2 = \frac{N!}{(N-X_2N)!\ (X_2N)!} \tag{28}$$

Ω_3 is the number of distinguishable ways of arranging X_3N potassium ions over the remaining $(N-X_2N)$ available positions.

$$\Omega_3 = \frac{(N-X_2N)!}{(N-X_2N-X_3N)!\,(X_3N)!} \tag{29}$$

and Ω_1 is the number of distinguishable ways of arranging the αX_1N "bonded" silver ion over the remaining $(N-X_2N-X_3N)$ available positions.

$$\Omega_1 = \frac{(N-X_2N-X_3N)!}{(N-X_2N-X_3N-\alpha X_1N)!\ (\alpha X_1N)!} \tag{30}$$

There is no freedom with regard to the distribution of the free silver ions or the chloride ions. Simplifying equations (27,28,29 and 30) yields for 1 mole of solution.

$$\Omega = \frac{N!}{(X_2N)!\ ((1-\alpha)X_1N)!\ (\alpha X_1N)!\,(X_3N)!} \tag{31}$$

The total configurational entropy of the ternary solution is determined by applying Boltzmann's equation:

$$S_{ternary} = k \ln \Omega \tag{32}$$

Applying the Stirling approximation

$$\ln (N!) = \ln \prod_{i=1}^{N} i = \sum_{i=1}^{N} \ln i = \int_{i=1}^{N} \ln i \, di$$

$$= N \ln N - N \qquad \text{for large N} \tag{33}$$

and simplifying

$$S_{ternary} = -R(X_2 \ln X_2 + X_3 \ln X_3 + aX_1 \ln aX_1 + (1-a)\, X_1 \ln (1-a)X_1) \tag{34}$$

The configurational entropy for a mole of pure silver chloride is, by similar reasoning:

$$S^{o}_{AgCl} = -R\,(a^{o} \ln a^{o} + (1-a^{o}) \ln (1-a^{o})) \tag{35}$$

where a^{o} is a fraction of silver that exists as Ag^{+} in pure molten silver chloride. If the configurational entropy of a mole of the lithium chloride and potassium chloride melt is simply given by:

$$S_{(Li,K)Cl} = -R\left(\frac{X_2}{X_2+X_3} \ln \frac{X_2}{X_2+X_3} + \frac{X_3}{X_2+X_3} \ln \frac{X_3}{X_2+X_3}\right) \tag{36}$$

wherein it is assumed that the lithium and potassium ions are randomly mixed, then it is possible to evaluate the configurational entropy change for the mixing process given by equation (26).

$$\Delta S = S_{ternary} - X_1\, S^{o}_{AgCl} - (1-X_1)\, S_{(Li,K)Cl} \tag{37}$$

This will be regarded as the total entropy change for the process; that is, vibrational entropy changes will be neglected. Accordingly, it is possible to express ΔS in terms of a and a^{o}.

The enthalpy change for the reaction expressed by equation (26) is assumed to be mainly the result of an increase or decrease in the fraction of silver that is "bonded". A change in this fraction is expected as the character of the melt is altered by changes in the relative population of alkali cations.

Let ϵ_1, ϵ_2, ϵ_3 refer to the energy per mole associated with the process

$$Ag^{+} + \quad Ag^{+}$$

in pure silver chloride, pure lithium chloride and pure potassium chloride respectively. Further, suppose that in the ternary solution as a first approximation, the energy for this process is given by:

$$\epsilon = X_1\epsilon_1 + X_2\epsilon_2 + X_3\epsilon_3 \tag{38}$$

Regarding the energy liberated during the formation of the solution as being entirely due to the energy associated with a change in α, and neglecting the formal distinction between enthalpy and internal energy because the volume change on mixing is small, the enthalpy change per mole of solution for reaction (26) is given by:

$$\Delta H = \alpha X_1 (X_1 \epsilon_1 + X_2 \epsilon_2 + X_3 \epsilon_3) - \alpha^0 X_1 \epsilon_1 \tag{39}$$

The value of α at any composition is that which results in the minimum free energy of the solution:

$$\frac{\partial G}{\partial \alpha} = \frac{\partial H}{\partial \alpha} - T\frac{\partial S}{\partial \alpha} = 0 \tag{40}$$

$$\frac{\partial H}{\partial \alpha} = X_1^2 \epsilon_1 + X_1X_2 \epsilon_2 + X_1X_3 \epsilon_3 \tag{41}$$

$$\frac{\partial S}{\partial \alpha} = -RX_1 \ln \frac{\alpha}{(1-\alpha)} \tag{42}$$

Accordingly:

$$X_1^2 \epsilon_1 + X_1X_2 \epsilon_2 + X_1X_3 \epsilon_3 + RTX_1 \ln \frac{\alpha}{(1-\alpha)} = 0 \tag{43}$$

Rearranging:

$$\alpha = \frac{\prod_{i=1}^{3}\left(\exp\left[\frac{-X_i \epsilon_i}{RT}\right]\right)}{1 + \prod_{i=1}^{3}\left(\exp\left[\frac{-X_i \epsilon_i}{RT}\right]\right)} \tag{44}$$

By similar reasoning α^0 may be found.

$$\alpha^0 = \frac{\exp\left[\frac{-\epsilon_1}{RT}\right]}{\left(1 + \exp\left[\frac{-\epsilon_1}{RT}\right]\right)} \tag{45}$$

Accordingly ΔG for reaction (26), as well as ΔH and ΔS, is determined entirely by the values assigned to ϵ_1, ϵ_2, and ϵ_3. These parameters are, of course, adjustable for the purposes of fitting the experimentally observed behaviour of the system. However, to be consistent with the previous work of Pelton,* ϵ_1 and ϵ_3 must have the values -3500 and -5500 cal.g.mole^{-1} respectively. Thus ϵ_2 was treated as the only adjustable number in fitting the experimental data reported in the previous section. That experiment did not yield direct measurements of ΔG, ΔH or ΔS for the reaction in Equation (26); rather, relative partial molar properties of silver chloride were measured. However, these are related to the properties of reaction (26). Reference to Figure 15 will co-ordinate the following discussion of this relationship.

The plane tangent to the ternary integral free energy of mixing surface at composition X intersects the silver chloride edge of the right triangular prism thus defining $\Delta\bar{G}_{AgCl}$ at the composition X. It may be shown that along the composition path ψ that,

$$\Delta\bar{G}_{AgCl} = -\Lambda \frac{d\Delta Gmix}{d\Lambda} + \Delta Gmix \qquad (46)$$

But this is equivalent to

$$\Delta\bar{G}_{AgCl} = -\Lambda \frac{d\,(\Delta Gmix - \Lambda\,(\Delta G^{*}mix))}{d\Lambda} + (\Delta Gmix - \Lambda\Delta G^{*}mix) \qquad (47)$$

where ΔG^{*}_{mix} is the molar integral free energy of mixing of the lithium chloride potassium chloride melt with the composition falling on line ψ. The term (ΔG mix - $\Lambda\Delta G^{*}$ mix) may be recognized as the ΔG referred to previously in connection with equation (26).

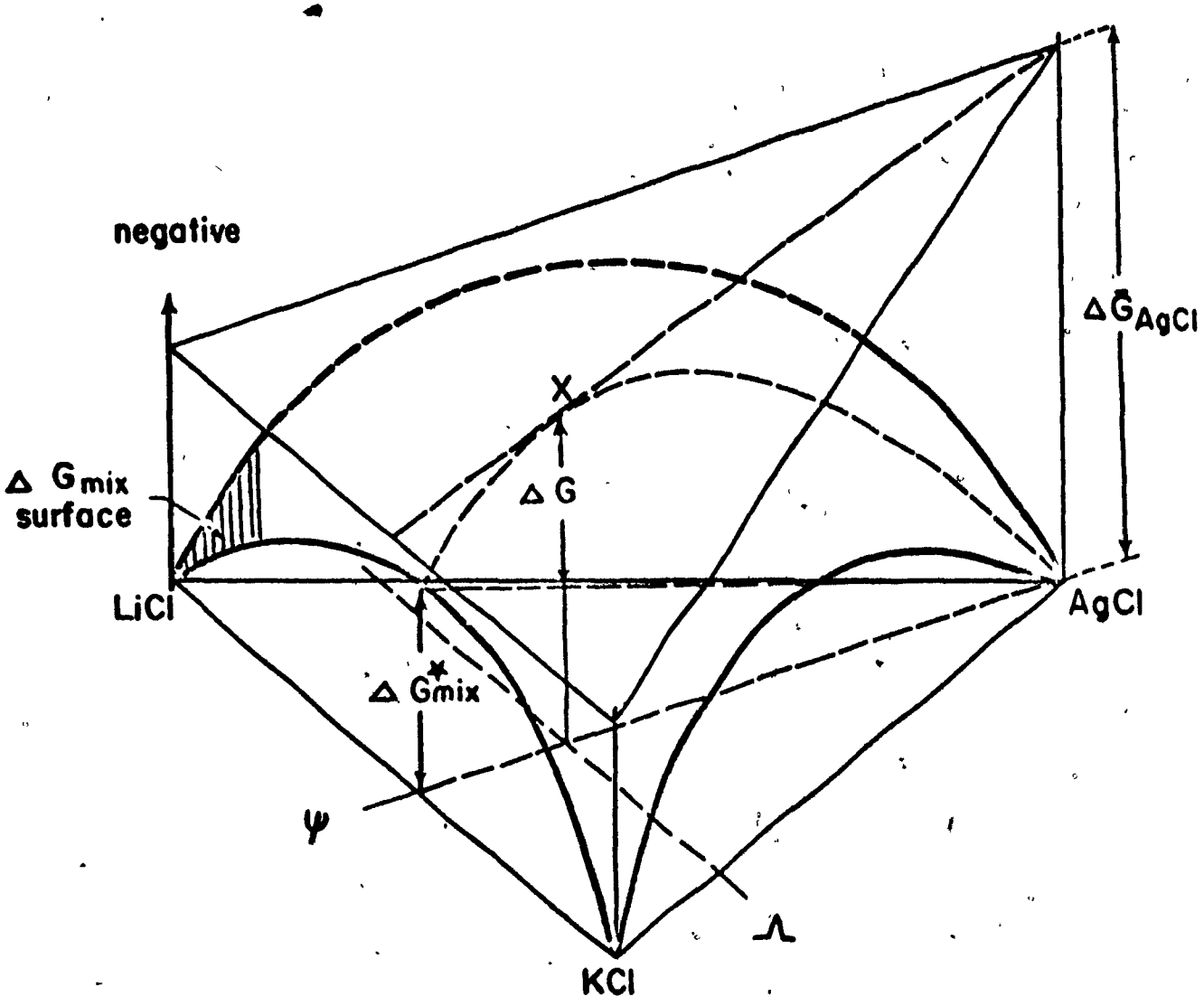

FIGURE 15. Diagram indicating relationship between partial and integral properties.

By the application of equation (47) it is possible to establish $\Delta\bar{G}_{AgCl}$ from the dual bonding model that has been developed to relate to the thermodynamic properties for reaction (26).

With a value of -500 cal/g mole for ϵ_2, $\Delta\bar{G}_{AgCl}$ was calculated and the activity at 500°C was determined, by the following equation:

$$a_{AgCl} = \exp \frac{\Delta\bar{G}_{AgCl}}{RT} \qquad (48)$$

The activity isotherm appears on the transparent overlay in Figure 16 . In register on the following page appears a duplicate of Figure 14 . To further the comparison between the theoretical and actual properties, $\Delta\bar{G}^E_{AgCl}$ surface was calculated using the model. This appears on the transparent overlay in Figure 17 . In register, on the following page, is a duplicate of Figure 13 representing the experimentally observed behaviour.

It is possible to compare the calculated and experimental relative partial enthalpy and entropy. Calculated values for these properties are shown in Appendix E. It should be realized that relative partial enthalpy and entropy were not determined with high precision and the comparison might be misleading; in addition, the model shows some inadequacy even in the activity and excess free energy and so limitations of the model are much more apparent in the sensitive enthalpy and entropy functions.

The major drawback of this treatment probably relates to equation (36) which assumes random mixing of lithium and potassium ions. In view of the relatively large difference in ionic radius this assumption may not be entirely correct. It is possible to pursue this point more fully; in spite of the fact that, entropies of mixing for the lithium and potassium chloride have not been measured.

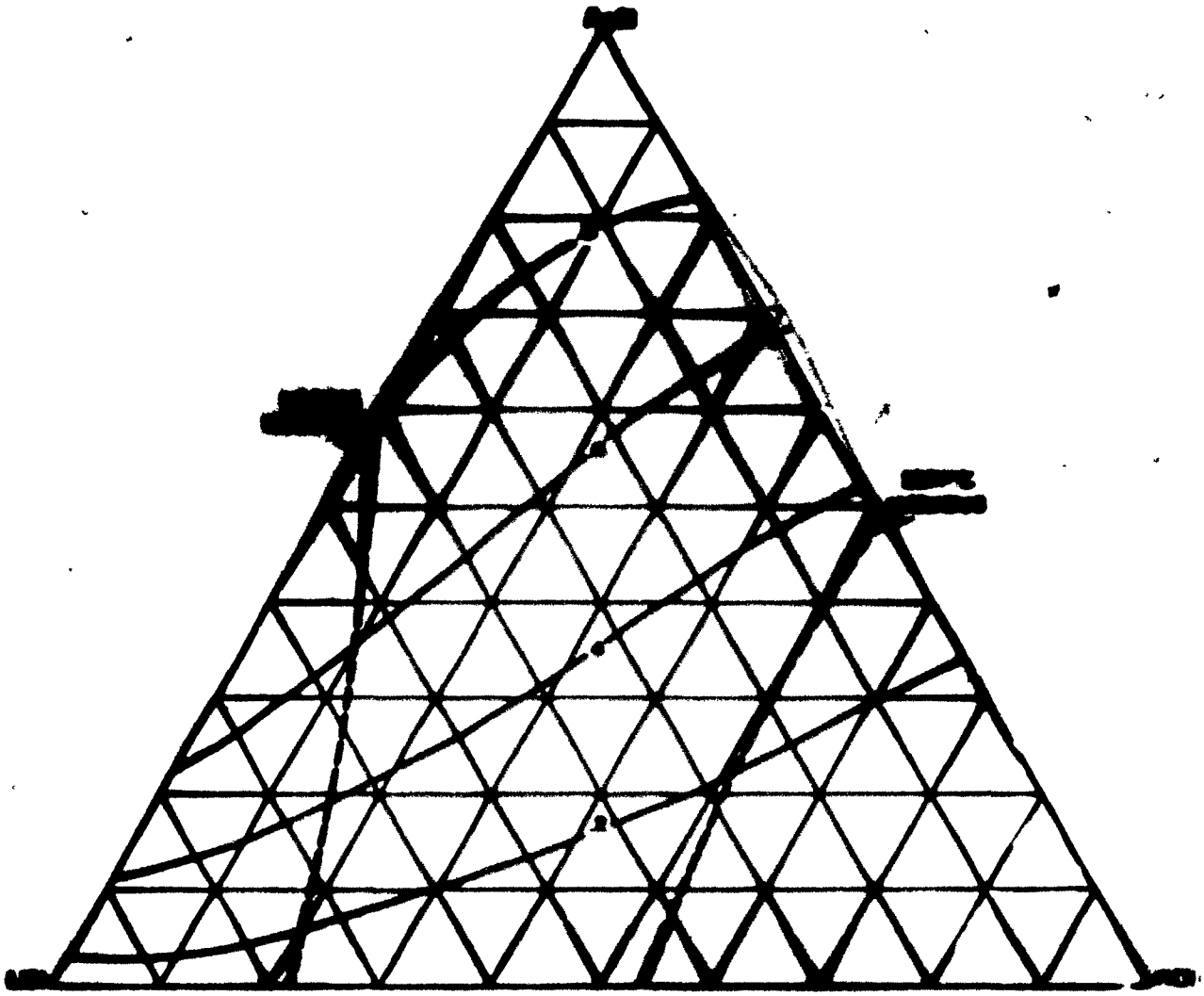

FIGURE 36. [illegible]

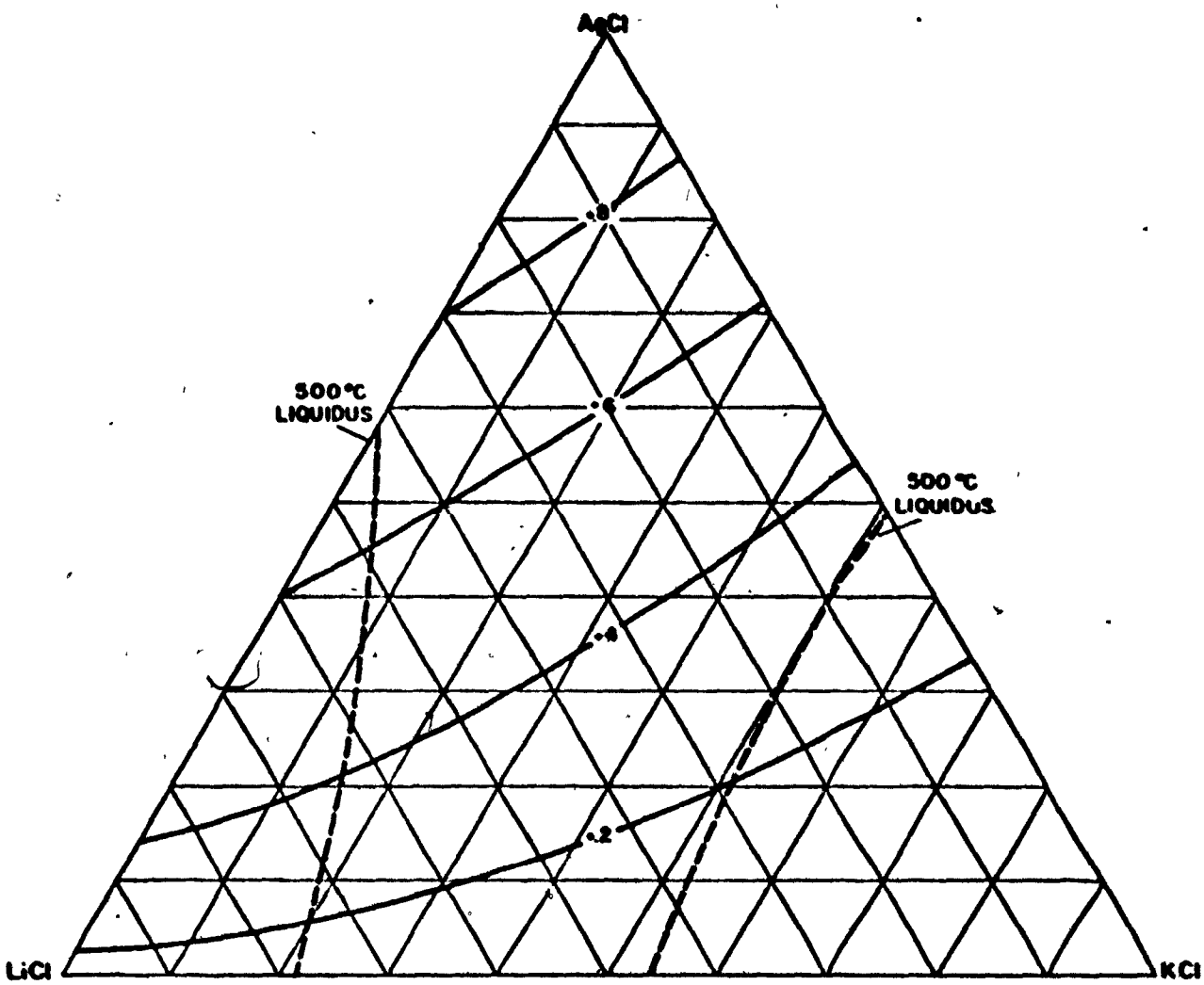

FIGURE 14. Activity isotherm for AgCl at 500°C determined experimentally.

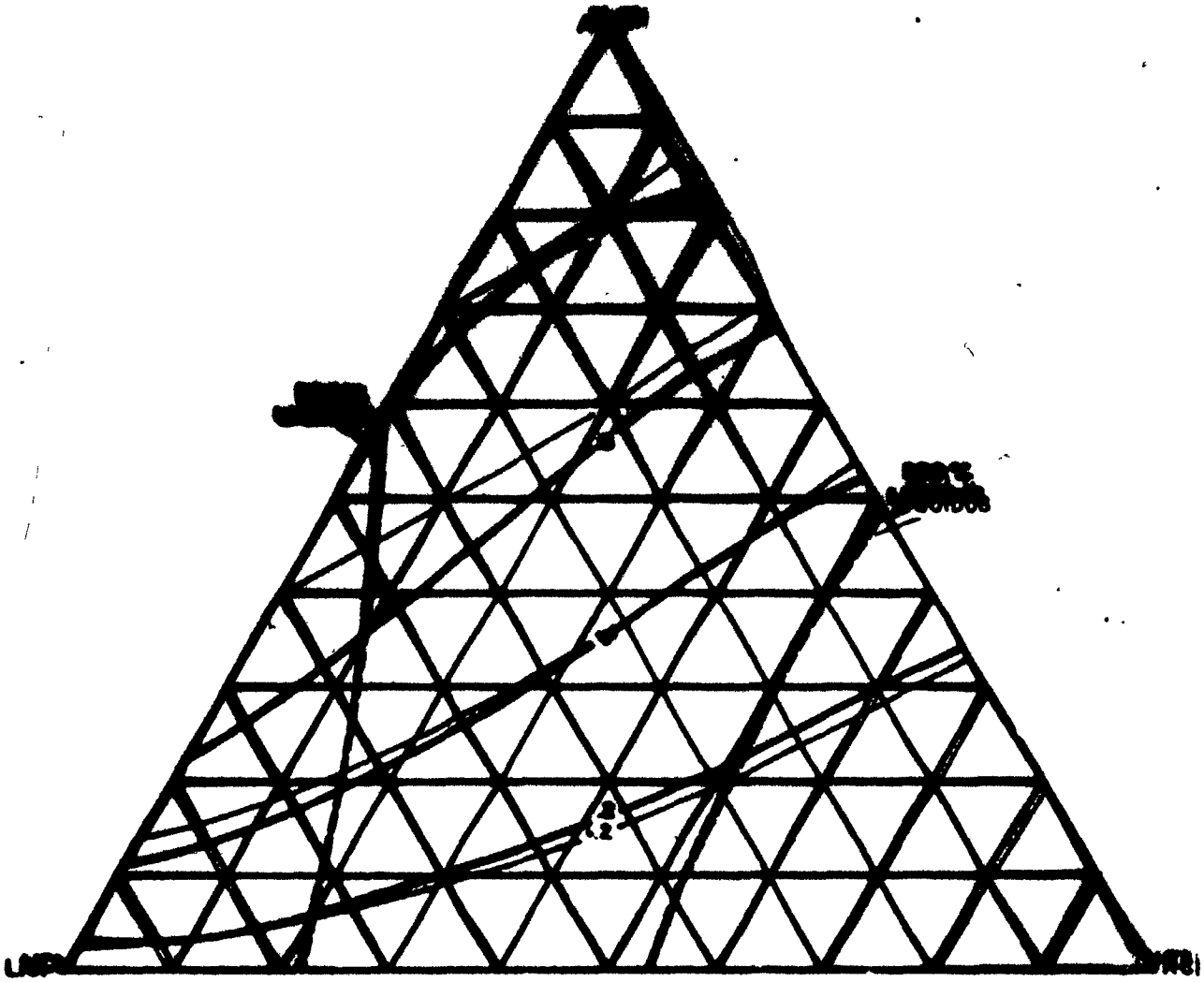

FIGURE 16. [illegible] Isotherm for AgCl at 500°C as Calculated Using the [illegible]

FIGURE 14. [illegible] Isotherm for AgCl at 500°C determined experimentally.

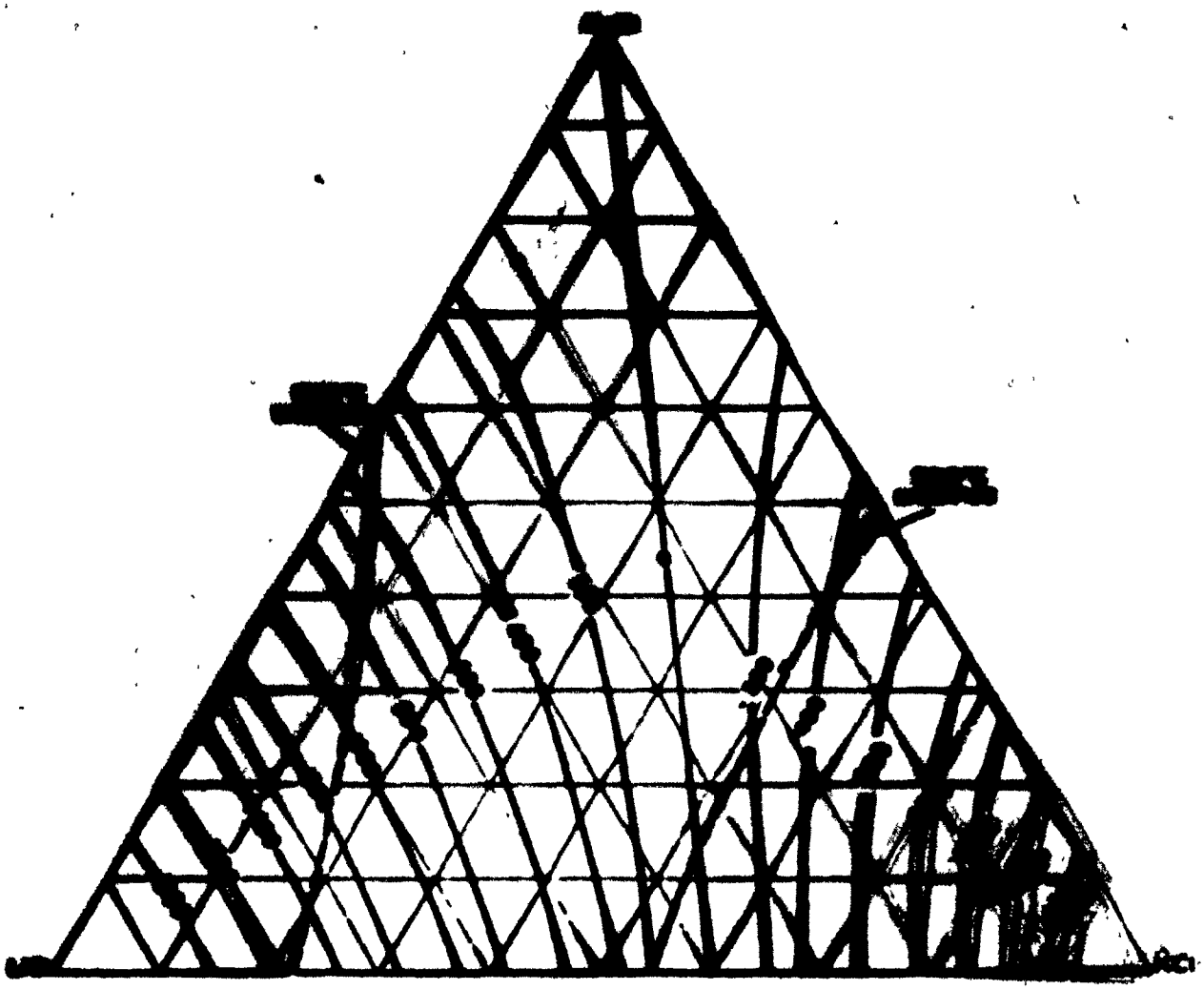

FIGURE 12. [illegible]

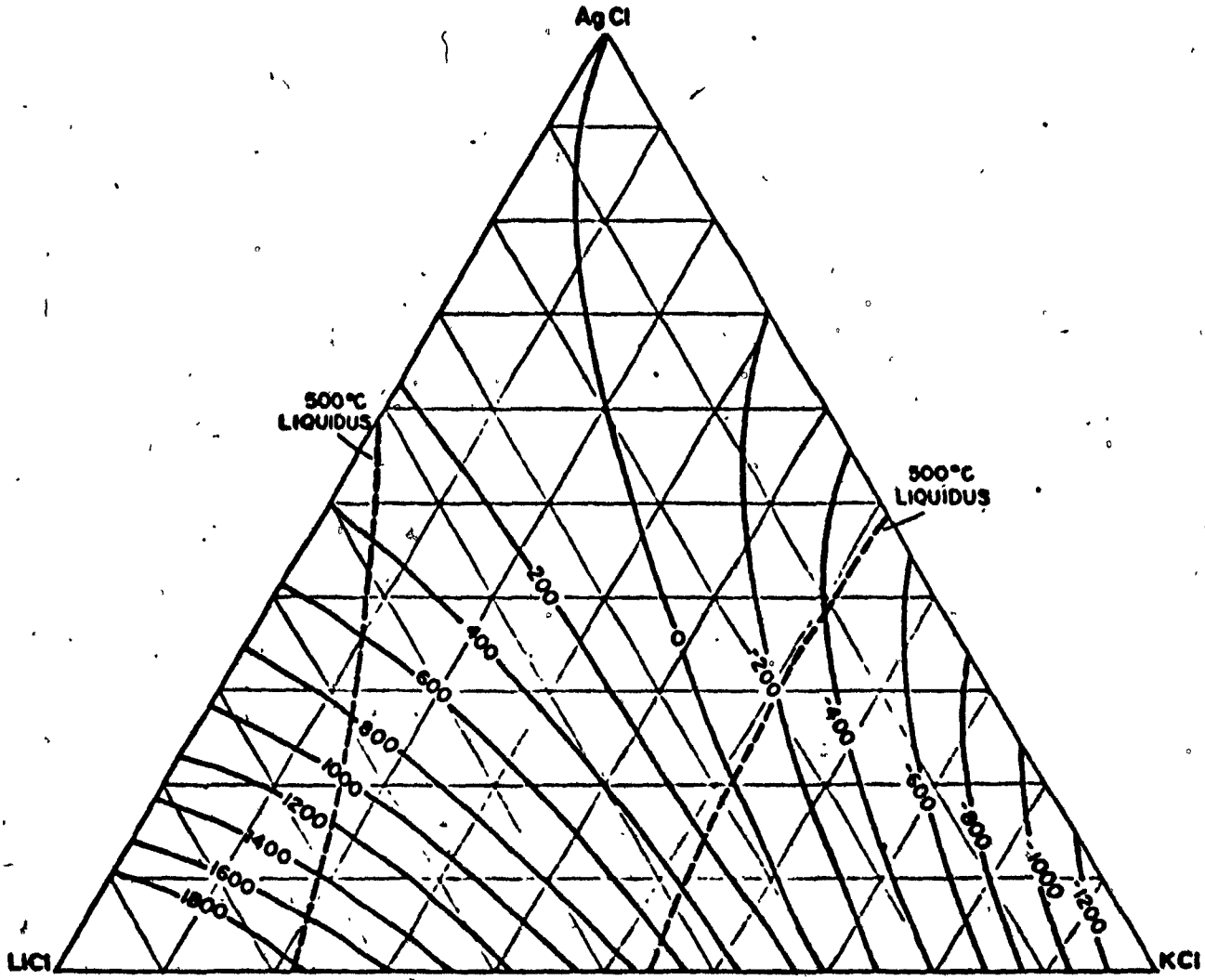

FIGURE 13. ΔG^E of AgCl at 500°C in the AgCl-LiCl-KCl system. The units are cal./g. mole.

Properties of the Lithium Chloride - Potassium Chloride Binary Melts

It is not possible to establish the thermochemical properties of lithium chloride - potassium chloride melts using the thermochemical technique employed in this research owing to the similar electrochemical behaviour of lithium and potassium. It is, however, possible to calculate approximate values for the free energy and entropy of mixing from the phase diagram and enthalpy of mixing determinations which together constitute the only reliable data for this system.

This calculation is best described with reference to Figure 18. In the upper portion of this figure in solid lines appears the accepted form of the lithium chloride, potassium chloride phase diagram (25). In the lower portion of this figure an integral free energy of mixing isotherm appears. To this curve may be assigned the general equation

$$\Delta G^{*}_{mix} = \Delta H^{*}_{mix} - T\Delta S^{*}_{mix} \qquad (49)$$

from the calorimetric measurements of Marchidan and Telea[24].

ΔH^{*}_{mix} is given by:

$$\Delta H^{*}_{mix} = -1405\,\Psi + 1821\,\Psi^{2} - 416\,\Psi^{3} \qquad (50)$$

where Ψ is the mole fraction of potassium chloride in this instance.

ΔH^{*}_{mix} is here regarded as being independent of temperature. Let

$$\Delta S^{*}_{mix} = \Delta S^{*}_{ideal} + \left\{-c\Psi - d\Psi + c\Psi^{2} + d\Psi^{3}\right\} \qquad (51)$$

The final grouping in braces represent the assumed form of the integral excess entropy.

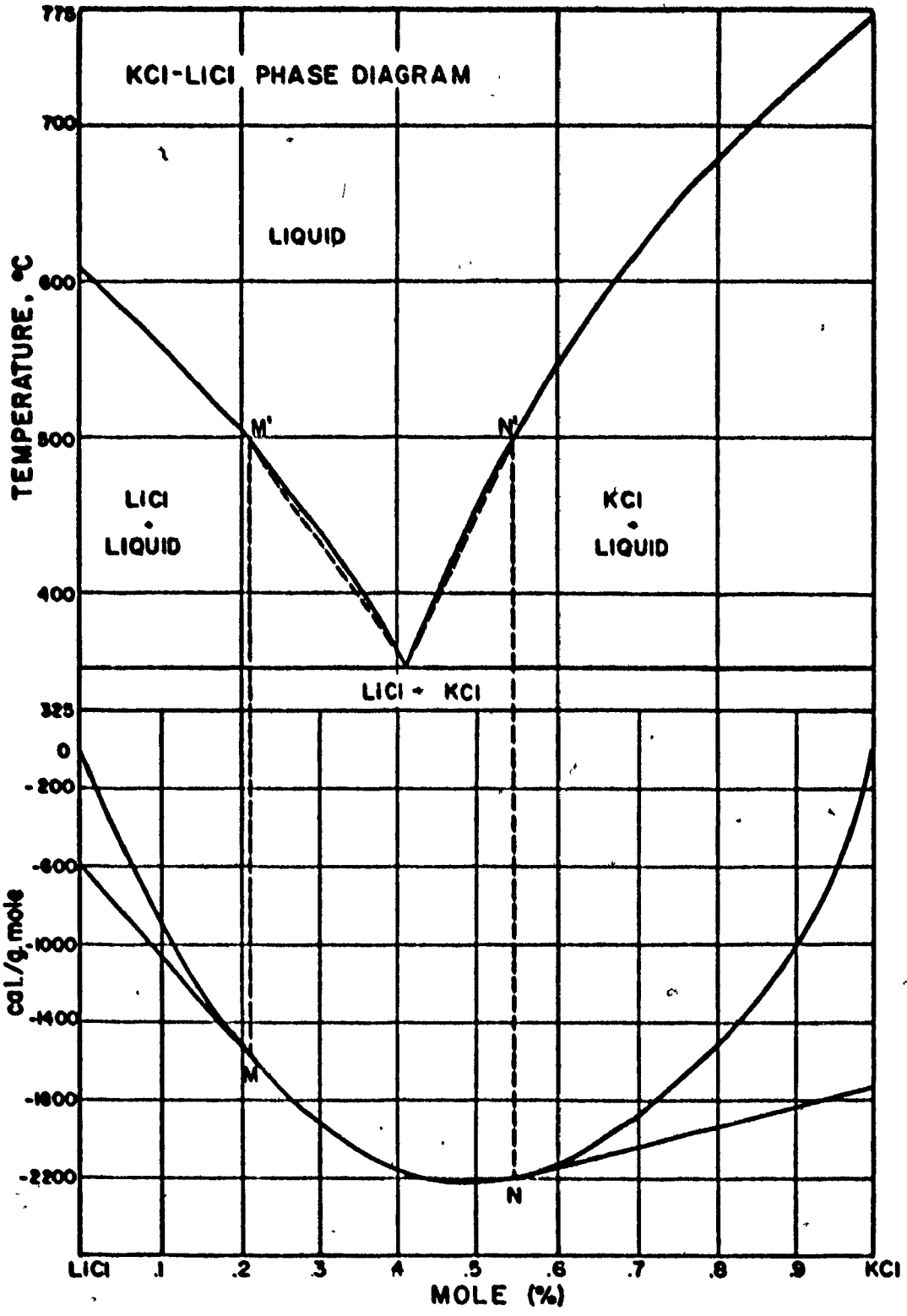

FIGURE 18. Phase diagram of KCl-LiCl and free energy curve at 500°C.

The constants c and d may be determined as follows. When solid lithium chloride is in equilibrium with a lithium chloride - potassium chloride liquid then,

$$(\bar{G}_2)_{(1)} = (\bar{G}_2)_{(s)} = (G^o_2)_{(s)} \tag{52}$$

Subtracting from both sides $(G^o_2)_{(1)}$

$$(\bar{G}_2)_{(1)} - (G^o_2)_{(1)} = (G^o_2)_{(s)} - (G^o_2)_{(1)} \tag{53}$$

It follows that

$$(\Delta\bar{G}_2)_{(1)} = - (\Delta G_2)_{(f)} \tag{54}$$

the subscript (f) indicating fusion.

Similarly for KCl saturated melts

$$(\Delta\bar{G}_3)_{(1)} = - (\Delta G_3)_{(f)} \tag{55}$$

The melt may be simultaneously saturated with lithium chloride and potassium chloride at the eutectic temperature. Since

$$(\Delta\bar{G}_2)_{(1)} = - \psi \frac{d\Delta G^*_{mix}}{d\psi} + \Delta G^*_{mix} \tag{56}$$

and a similar equation applies to $(\Delta\bar{G}_3)$ it follows that at the eutectic temperature and composition the tangent drawn to ΔG^*_{mix} curve must intersect at the lithium chloride and potassium chloride sides of the free energy diagram at minus the free energy of fusion of the components at this temperature.

The free energy of fusion of lithium chloride and potassium chloride may be calculated from the enthapy of fusion and difference in heat capacity between solid and liquid phases[15].

$$(\Delta G)_{(f)} = - \int_{T_{(f)}}^{T} \Delta S_{(f)}\, dT \qquad (57)$$

where

$$\Delta S_{(f)} = \frac{\Delta H_{(f)}}{T_{(f)}} + \int_{T_{(f)}}^{T} \frac{(Cp)_{(l)} - (Cp)_{(s)}}{T}\, dT \qquad (58)$$

it follows that

$$(\Delta G_{(f)})_2 = 1053.5 + 43.46T + .0032T^2 - 7.00\ T \ln T \qquad (59)$$

$$(\Delta G_{(f)})_3 = 2721.0 + 37.28T + .0026T^2 + \frac{38500}{T} - 6.11T \ln T \qquad (60)$$

where the results are expressed in cal gm mole^{-1}. Accordingly, at the eutectic temperature and composition

$$\Delta G^{*}_{mix} = (1-\forall)\ (\Delta G_{(f)})_2 + \forall (\Delta G_{(f)})_3 \qquad (61)$$

and

$$\frac{d\Delta G^{*}_{mix}}{d\forall} = (\Delta G_{(f)})_3 - (\Delta G_{(f)})_2 \qquad (62)$$

Solving these equations c and d were determined as -2.70 and -1.17 cal g mole^{-1} K^{-1}.

The adequacy of this procedure for estimating the entropy and free energy of mixing may be judged from an examination of the upper part of Figure 18 wherein is shown the potassium chloride and lithium chloride liquidi as dashed lines consistent with the calculated c and d values in the entropy of mixing expression. The procedure involved in this calculation may be understood with reference to the lower part of Figure 18. The points of tangency M and N in the lower figure are the liquidus points M' and N' in the upper figure.

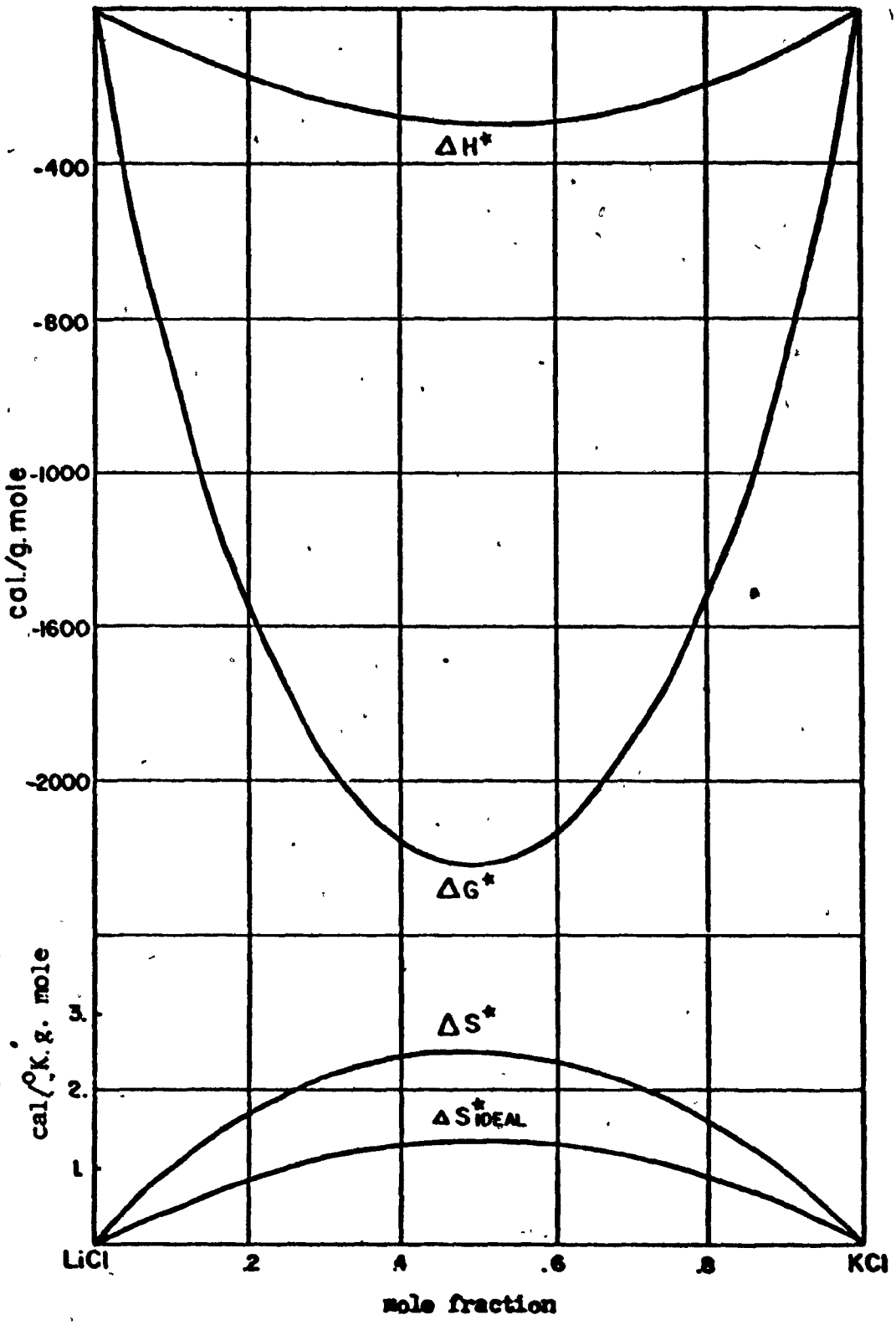

FIGURE 19. Integral properties of mixing of KCl and LiCl at 500°C.

The behaviour of the enthalpy of mixing, entropy of mixing and free energy of mixing is displayed in Figure 19 . The noteworthy point is the large positive excess entropy exhibited in this binary system. Considering the nature of the calculations leading to these figures and the thermochemical data involved, the entropy of mixing should be regarded as approximate. However, the conclusion that ΔS^E is significantly positive appears certain. It is probable, for this reason, that this entropy effect, ignored in the development of the dual bonding model for ternary solutions, is responsible for the discrepancies evident in Figures 16 and 17 . Nevertheless, in spite of these discrepancies, the dual bonding model may be a useful way of understanding the behaviour of the thermochemical properties in silver chloride ternary melts. It will at least, semi-quantitatively generate activity isotherms with a minimum number of parameters (only three) to which must be assigned arbitrary values.

The estimated properties of the lithium chloride - potassium chloride binary melt make possible the calculation of the ternary free energy of mixing, enthalpy of mixing and entropy of mixing since a boundary condition for Gibbs-Duhem integration is available. These properties and discussion of the calculations appear in Appendix D.

Application to Electrodeposition

It is possible to speculate on the significance of the dual bonding model with respect to the problem of obtaining smooth cathodic deposits from fused chloride melts briefly referred to in the introduction. In this connection it is worthwhile to review the factors thought to favour a smooth deposit from aqueous solutions.

Consider the deposit of silver from an aqueous solution. Silver deposited from nitrate solutions in silver refining cells constitutes a classic example of a dendritic and non-coherent deposit. The high concentration of free silver ions adjacent to the cathode aided by the action of the electric field favours growth rather than nucleation. That is to say, an abundance of dischargeable ions would make it energetically unfavourable to overcome interfacial energy effects associated with the establishment of new locations where silver may be deposited. At the other extreme silver deposited from aqueous cyanide solutions is at least smooth in a macroscopic sense. In such solutions silver exists almost entirely as a complex anion in the presence of an excess of alkali cyanide. Thus the action of the electric field during deposition is such as to transport the complex silver ions away from the cathode. The supply of $Ag(CN)_2^-$ complex ions to the cathode is controlled entirely by diffusion processes. At the current densities normally employed this situation might be expected to favour nucleation rather than growth on established cathodic sites.

In the case of deposition of silver from alkali chloride melts reasoning similar to the above would suggest that additions of alkali chloride that favours the reduction in the quantity of free silver would tend to promote smooth deposits. Pelton has shown that in the presence of high concentrations of cesium chloride the α referred to in the dual bonding model is largest. This conclusion is based on its success in rationalizing precisely measured thermodynamic properties of AgCl alkali chloride binary melts from sodium through cesium and which has as a result

of the present research been shown to be semi-quantitatively applicable to ternary melts.

CONCLUSION

The thermodynamic properties of molten silver chloride, lithium chloride, potassium chloride were studied using a silver chloride formation cell employing a chlorine electrode of unusual design which facilitated measurements in ternary melts.

The data were treated by analytical methods resulting in the generation of activity, the relative partial molar excess free energy, the relative partial molar enthalpy and the relative partial molar entropy for silver chloride at 500°C.

The measured properties were interpreted with the aid of a melt model which presupposed the existence of free silver ions as well as those "bonded" to adjacent chloride ions. With three adjustable parameters it was possible to account, semi-quantitatively, for the behaviour and activity of silver. This information is regarded as being significant in understanding the phenomena associated with dendritic electrodeposits from chloride melts.

REFERENCES

1. J.H. FEARON, "Chemical Technology", Vol. 3, Barnes and Noble, 252, (1970).

2. J. GUION, M. BLANDER, D. HENGSTENBERG, and K. HAGEMARK, J. Phys. Chem., 72, 2086, (1968).

3. A.D. PELTON, S.N. FLENGAS, J. Electrochem, Soc., 118, 1307, (1971).

4. S.N. FLENGAS and T.R. INGRAHAM, J. Electrochem. Soc., 106, 714, (1959).

5. H.A. LAITINEN, W.S. FERGUSON and R.A. OSTERYOUNG, J. Electrochem. Soc., 104, 516, (1957).

6. I.M. KOLTHOFF and E.B. SANDELL, "Textbook of Quantitative Inorganic Analysis", 3rd Ed., MacMillan, (1952).

7. I.M. KOLTHOFF and P.J. ELVING, "Treatise on Analytical Chemistry", John Wiley & Sons, New York, Pt. 2, Vol. 1, (1961).

8. A.D. PELTON, S.N. FLENGAS, J. Electrochem. Soc., 117, 1130, (1970).

9. S. SIENDEROFF and G.W. MELLORS, Rev. Sc. Instr., 29, 151, (1968).

10. M.B. PANISH, F.F. BLANKENSHIP, W.R. GRIMES and R.F. NEWTON, J. Phys. Chem., 62, 1325, (1958).

11. J. LEONARDI and J. BRENET, Compt. Rend., 261, 116, (1965).

12. I.G. MURGULESCU and S. STERNBERG, Rev. Chem. Acad. Rep., Pop. Rou., 2, 251, (1957).

13. E.J. SALSTROM, J. Am. Chem. Soc., 56, 1272, (1934).

14. J. HAMER, J. Electroanal. Chem., 10, 140, (1965).

15. O. KUBASHEWSKI and E.L. EVANS and C.B. ALCOCK, "Metallurgical Thermochemistry", Pergamon Press, 4th Edition, (1967).

16. W.T. THOMPSON and S.N. FLENGAS, Can. J. Chem., 49, 1550, (1971).

17. A.D. PELTON, Ph.D. Thesis, University of Toronto, (1970).

18. M.B. PANISH, R.F. NEWTON, W.R. GRIMES and F.F. BLANKENSHIP, J. Phys. Chem., 63, 668, (1959).

19. E.W. DEMING, Metallurgical Transactions, 3, 495, (1972).

20. A.D. PELTON and W.T. THOMPSON, Can. J. Chem., 48, 10, (1970).

21. J. BRAUNSTEIN and M. BLANDER, J. Phys. Chem., 64, 10, (1959).

22. F.R. DUKE and H.M. GARFINKEL, J. Phys. Chem., 65, 461, (1961).

23. A.S. KUCHARSKI and S.N. FLENGAS, Can. J. Chem., 49, 3971, (1971).

24. D. MARCHIDAN, C. TELEA, Rev. Roum. Chem. 13, 291, (1968).

25. E. ELCHARDUS and P. LAFFITTE, Bull. Soc. Chim., France, 51, 1572, (1932).

26. T.B. REDDY, J. Electrochem. Soc., 113, 117, (1966).

27. A.D. PELTON, S.N. FLENGAS, Can. J. Chem., 47, 2283, (1969).

APPENDIX A

LIST OF SYMBOLS

List of Symbols

a	fraction of bonded silver ions in ternary melt
a^o	fraction of bonded silver ions in a pure silver chloride melt
a	activity; regression coefficient
b	regression coefficient
c	constant
d	constant
E	measured electromotive force
E^o	standard electromotive force
E^*	electromotive force corrected to 1 atmosphere chlorine pressure
F	Faraday constant
G^o	standard molar Gibbs free energy
ΔG^E	integral excess Gibbs free energy
ΔG_i^E	partial molar excess Gibbs free energy of component i
$\Delta G_{(f)}$	Gibbs free energy of fusion
H^o	standard molar enthalpy
ΔH_{mix}	integral enthalpy of mixing
ΔH_i	relative partial molar enthalpy of component i
k	Boltzmann's constant
Λ	composition variable
N	Avogadro's number
P	pressure
R	ideal gas constant

S^{o}	standard molar entropy
ΔS	integral entropy of mixing
$\Delta \bar{S}_i$	relative partial molar entropy of component i
ΔS^{E}	integral excess entropy
T	absolute temperature
Y	composition variable
Ω	multiplicity
X	mole fraction

APPENDIX B

LIST OF MATERIALS

List of Materials

Lithium Chloride	Reagent Grade	Fisher
Potassium Chloride	Reagent Grade	Fisher
Silver Chloride	Reagent Grade	Baker
Argon	Purified Technical Grade	Canadian Liquid Air
Anhydrous HCl	Electronic Grade	Canadian Liquid Air
Chlorine Gas	Purified Technical Grade	Canadian Liquid Air
Graphite Rod	Grade SPK	National Carbon
Silver Wire	99.999%	Fisher
Antimony	59 Grade	Cominco
Lead	59 Grade	Cominco

APPENDIX C

RESULTS OF ELECTROMOTIVE FORCE EXPERIMENTS

Results of Electromotive Force Experiments

The data used for the binary system AgCl-LiCl were taken from Panish et al.[18] and the data used for the binary system AgCl-KCl were taken from Pelton[17]. The experimental results for the ternary system are listed in the following pages.

E(mv) = Experimental e.m.f. reading.

E^*(mv) = e.m.f. reading which has been corrected to 1 standard atmosphere of Cl_2. The thermocouple correction between the silver and carbon electrode has been added. (refer to page 16)

E^*_{calc}(mv) = The E^* calculated at various temperatures using the sigma interpolation. (refer to page 21)

Pure AgCl

Temp. (^{o}K)	P_{Cl_2} (Torr)	E(mv)	E^{*} (mv)	E_{calc} (mv)
755.0	765.2	901.6	903.7	903.6
738.8	764.5	906.6	908.6	908.3
758.3	764.0	900.3	902.5	902.7
780.0	764.1	894.0	896.4	896.4
788.2	763.8	891.7	894.2	894.1
773.1	763.9	896.4	898.8	898.4
807.6	764.0	886.0	888.7	888.6

MELT COMPOSITION A

COMPONENT	WEIGHT PERCENT	MOLE FRACTION
AgCl	53.8730	0.3085
LiCl	21.9970	0.4259
KCl	24.1300	0.2656

Temp. (^{o}K)	P_{Cl_2} (Torr)	E(mv)	E^{*} (mv)
717.6	785.9	968.0	968.9
766.0	785.6	954.8	956.2
738.2	780.4	962.5	963.8
699.3	778.1	971.0	972.1
675.1	777.8	977.1	978.0
665.0	778.1	979.6	980.4
683.7	778.1	974.8	975.8
719.7	778.3	967.1	968.4

MELT COMPOSITION B

COMPONENT	WEIGHT PERCENT	MOLE FRACTION
AgCl	44.7060	0.2360
LiCl	26.3680	0.4707
KCl	28.8950	0.2933

Temp(^{o}K)	P_{Cl_2} (Torr)	E(mv)	E^{*} (mv)
705.6	786.5	979.1	979.9
747.0	778.1	971.9	973.4
786.6	778.7	961.9	963.8
701.7	768.4	980.0	981.5
678.5	768.1	984.5	985.8
662.9	768.4	988.4	989.6
731.5	779.4	974.4	975.7
769.1	779.4	966.5	968.2

MELT COMPOSITION C

COMPONENT	WEIGHT PERCENT	MOLE FRACTION
AgCl	31.2200	0.1478
LiCl	32.7950	0.5248
KCL	35.9750	0.3274

Temp. (^{o}K)	P_{Cl_2} (Torr)	E(mv)	E* (mv)
743.4	790.8	991.4	992.4
747.5	790.8	990.6	991.6
749.0	791.3	991.0	992.0
784.5	791.3	984.1	985.4
731.9	792.3	994.1	994.9
706.0	793.1	998.0	998.6
666.5	790.7	1003.2	1003.6
666.2	789.4	1003.3	1003.7
701.6	788.6	997.7	998.4
733.6	789.1	993.3	994.2

MELT COMPOSITION D

COMPONENT	WEIGHT PERCENT	MOLE FRACTION
AgCl	25.0160	0.1130
LiCl	35.7580	0.5462
KCl	39.2260	0.3407

Temp. (^{o}K)	P_{Cl_2} (Torr)	E(mv)	E* (mv)
686.9	776.1	1007.7	1008.8
732.3	775.2	1003.3	1004.8
780.0	775.1	997.0	998.9
746.1	775.6	1001.1	1002.7
711.6	775.2	1006.0	1007.3
668.9	774.8	1013.1	1014.1
665.6	772.7	1012.0	1013.0
735.3	771.3	1003.1	1004.8

MELT COMPOSITION E

COMPONENT	WEIGHT PERCENT	MOLE FRACTION
AgCl	16.3360	0.0694
LiCl	39.8970	0.5731
KCl	43.7670	0.3575

Temp. (^{o}K)	P_{Cl_2} (Torr)	E(mv)	E* (mv)
684.5	780.7	1028.9	1029.8
668.9	780.5	1030.7	1031.5
712.8	771.6	1027.4	1028.9
748.5	771.0	1025.5	1027.3
756.9	771.4	1023.2	1025.1
704.1	771.9	1028.4	1029.8

MELT COMPOSITION F

COMPONENT	WEIGHT PERCENT	MOLE FRACTION
AgCl	9.8340	0.0400
LiCl	42.9980	0.5912
KCl	47.1680	0.3688

Temp. (^{o}K)	P_{Cl_2} (Torr)	E(mv)	E* (mv)
773.8	764.5	1059.5	1061.8
745.6	763.6	1057.1	1059.2
706.3	762.9	1054.9	1056.7
675.7	762.5	1053.6	1055.1
652.1	762.4	1051.0	1052.3

MELT COMPOSITION G

COMPONENT	WEIGHT PERCENT	MOLE FRACTION
AgCl	56.465	0.3321
LiCl	20.4760	0.4072
KCl	23.0590	0.2607

Temp. (^{o}K)	P_{Cl_2} (Torr)	E(mv)	E^{*} (mv)
791.4	764.6	953.6	956.1
802.0	764.6	951.1	953.7
784.3	764.6	954.4	956.8
763.0	764.1	958.3	960.5
741.5	763.9	962.0	964.0
727.0	763.9	964.9	966.8
744.2	763.7	961.7	963.8
767.5	763.7	957.2	959.5
788.1	762.4	953.5	956.1

MELT COMPOSITION H

COMPONENT	WEIGHT PERCENT	MOLE FRACTION
AgCl	48,7950	0.2676
LiCl	24.0850	0.4465
KCl	27.1200	0.2859

Temp. (^{o}K)	P_{Cl_2} (Torr)	E(mv)	E^{*} (mv)
791.3	773.3	961.5	963.6
776.7	773.1	964.4	966.4
757.4	772.6	968.1	969.9
739.6	772.6	971.4	973.1
757.4	770.1	967.9	969.8
783.5	770.1	962.8	964.9
779.9	769.9	964.4	966.6
799.2	768.6	961.5	963.9

MELT COMPOSITION I

COMPONENT	WEIGHT PERCENT	MOLE FRACTION
AgCl	82.9500	0.6534
LiCl	7.7020	0.2051
KCl	9.3480	0.1415

Temp.(^{o}K)	P_{Cl_2} (Torr)	E(mv)	E^{*} (mv)
806.5	766.4	916.0	918.6
773.7	766.7	924.5	926.7
758.4	766.9	928.8	930.9
756.8	767.8	928.4	930.5
740.7	768.2	933.1	935.0
755.0	767.8	929.6	931.6
769.3	767.8	926.1	928.2
791.5	767.8	920.6	923.0

MELT COMPOSITION J

COMPONENT	WEIGHT PERCENT	MOLE FRACTION
AgCl	75.4800	0.5439
LiCl	11.0770	0.2699
KCl	13.4430	0.1862

Temp.(^{o}K)	P_{Cl_2} (Torr)	E(mv)	E^{*} (mv)
766.7	770.1	931.4	933.4
786.9	770.3	926.3	928.5
802.6	770.1	923.6	926.0
780.9	769.9	928.0	930.2
759.8	769.9	933.1	935.1
748.7	770.0	936.5	938.4
724.7	769.8	941.6	943.2
738.9	769.8	938.1	939.9

MELT COMPOSITION K

COMPONENT	WEIGHT PERCENT	MOLE FRACTION
AgCl	64.8600	0.4169
LiCl	15.8750	0.3450
KCl	19.2650	0.2381

Temp. (^{o}K)	P_{Cl_2} (Torr)	E(mv)	E*(mv)
767.9	769.9	950.1	952.2
758.9	768.9	952.7	954.7
735.1	768.6	956.9	958.7
744.6	768.6	955.2	957.1
766.7	768.6	951.3	953.4
794.0	768.6	946.1	948.5
805.7	767.3	943.4	946.0
784.0	767.0	947.5	949.8

MELT COMPOSITION L

COMPONENT	WEIGHT PERCENT	MOLE FRACTION
AgCl	43.6450	0.2409
LiCl	20.0300	0.3737
KCl	36.3250	0.3854

Temp. (^{o}K)	P_{Cl_2} (Torr)	E(mv)	E*(mv)
753.3	771.2	977.9	979.8
735.7	771.1	981.1	982.7
767.7	770.4	975.5	977.5
790.6	770.4	972.0	974.3
802.8	770.9	970.3	972.6
778.5	771.2	974.1	976.2
760.2	771.5	976.7	978.6
741.5	773.6	979.4	981.0

MELT COMPOSITION M

COMPONENT	WEIGHT PERCENT	MOLE FRACTION
AgCl	16.7050	0.0759
LiCl	29.6050	0.4549
KCl	53.6900	0.4691

Temp. (^{o}K)	P_{Cl_2} (Torr)	E(mv)	E^{*} (mv)
755.6	770.9	1041.5	1043.4
726.9	770.8	1042.9	1044.5
748.0	770.5	1041.9	1043.7
775.8	770.5	1040.9	1043.0
806.2	773.0	1040.9	1043.2
776.8	773.0	1041.0	1043.0
763.6	773.0	1041.4	1043.3
745.5	773.0	1042.0	1043.7
731.8	773.0	1042.2	1043.8

APPENDIX D

CALCULATED INTEGRAL PROPERTIES

Calculated Integral Properties

When the partial molar excess properties of AgCl can be expressed with an expression of the type given in equation (19) and properties of the lithium chloride and potassium chloride melts are known, the integral excess properties may be determined from the following equation:[27]

$$\Delta G^E = \sum_{j=1} \sum_{k=0} e_{jk} \Lambda^j \psi^k \qquad (63)$$

where

$$e_{jk} = \frac{(a_{jk} - b_{jk}T)}{(1 - j)} \qquad \text{for } j > 2 \qquad (64)$$

The coefficients e_{jk} with $j = 0$ must all be zero since ΔG^E must be zero at pure silver chloride ($\Lambda = 0$). The coefficients e_{jk} with $j = 1$ may be determined from the condition that the integral excess free energy for the ternary system must reduce to that for the LiCl-KCl binary (refer to page 44) when $\Lambda = 1$.

When T is 773.16°K the integral excess free energy is given by the equation:

$$\Delta G^E = (1540.5 - 6629.89\psi + 2600.57\psi^2 + 488.3\psi^3)\Lambda + (-604.1 + 2292.7\psi + 726.7\psi^2)\Lambda^2 + (-936.3 - 59.6\psi + 581.2\psi^2)\Lambda^3 \qquad (65)$$

and in a similar manner ΔH_{mix} can be determined. Mechanically this involves dropping the $b_{jk}T$ term from equation (64).

Accordingly:

$$\Delta H_{mix} = (-338.37 + 292.64\psi - 1002.34\psi^2 - 416.29\psi^3)\Lambda + (+3895.69 - 3320.44\psi + 881.32\psi^2)\Lambda^2 + (-3557. + 1623.12\psi + 1941.99\psi^2)\Lambda^3 \qquad (66)$$

Similarly:

$$\Delta S^E = (-2.43 + 8.9\psi - 4.665\psi^2 - 1.17\psi^3)\Lambda + (+5.82 - 7.25\psi + .205\psi^2)\Lambda^2 + (-3.39 + 3.22\psi + 1.76\psi^2)\Lambda^3 \quad (67)$$

Equations (65, 66 and 67) for ΔG^E, ΔH_{mix} and ΔS^E are plotted on the Gibbs triangle in Figures 20, 21 and 22 .

It has been pointed out that the integral properties of a ternary system can be determined when the partial property of one component is known at all compositions in the system. However, this method requires that extremely accurate values of the partial properties be known in the region rich in that component. For practical purposes the method employed in the construction of Figures 20, 21 and 22 is the only suitable technique.

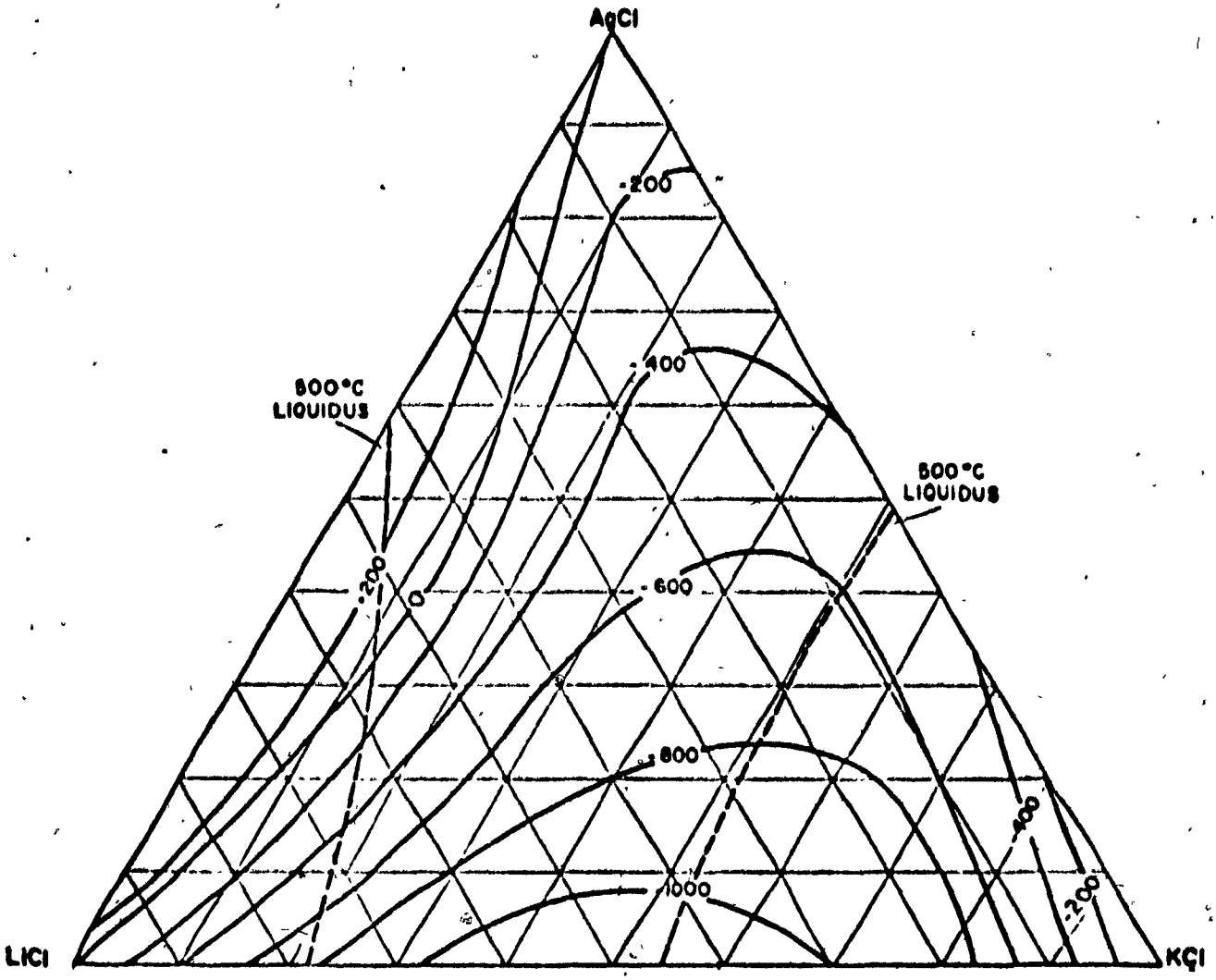

FIGURE 20. ΔG^{E}_{mix} of AgCl-LiCl-KCl at 500°C. The units are cal./g. mole.

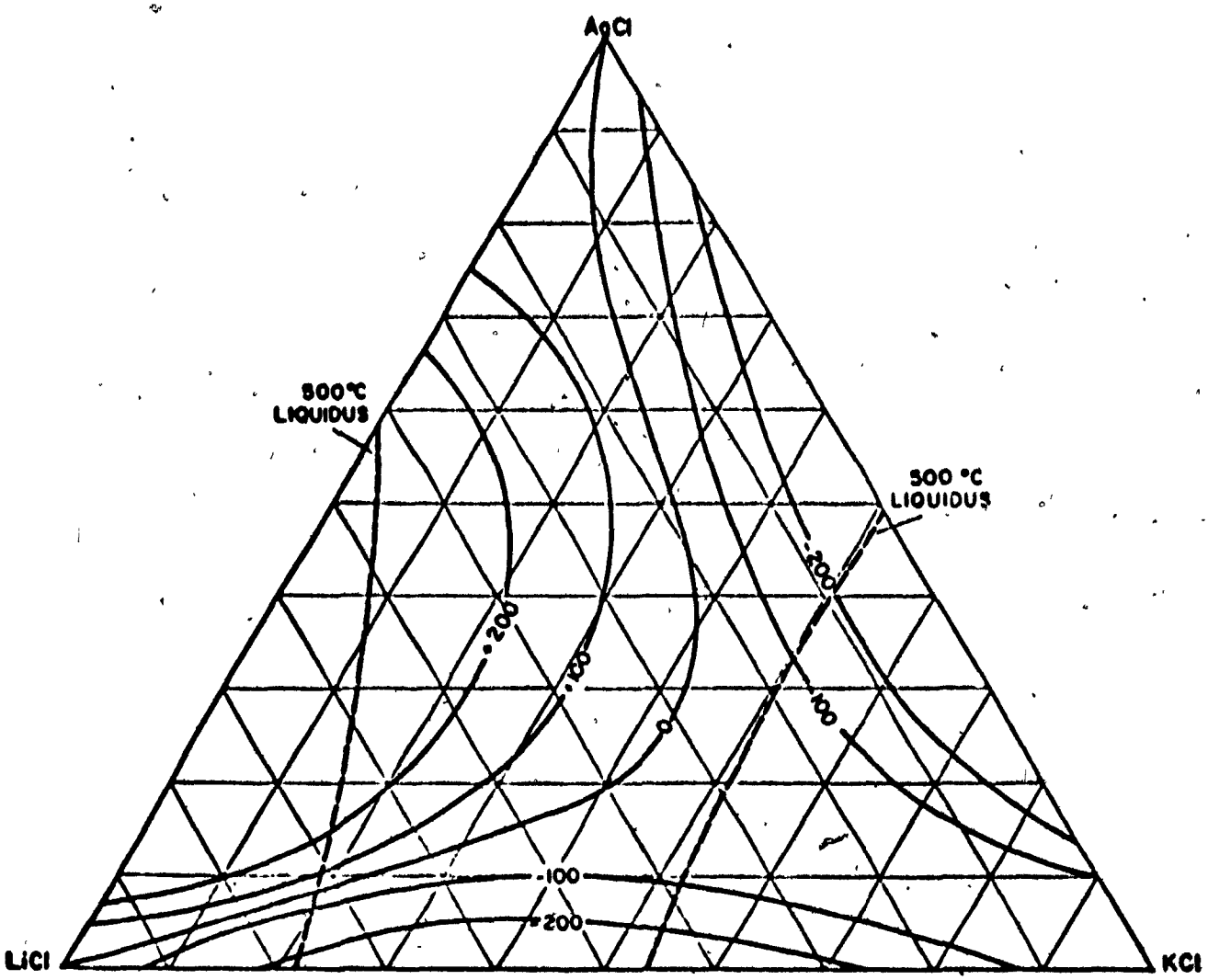

FIGURE 21. ΔH_{mix} of AgCl-LiCl-KCl.
The units are cal./g. mole.

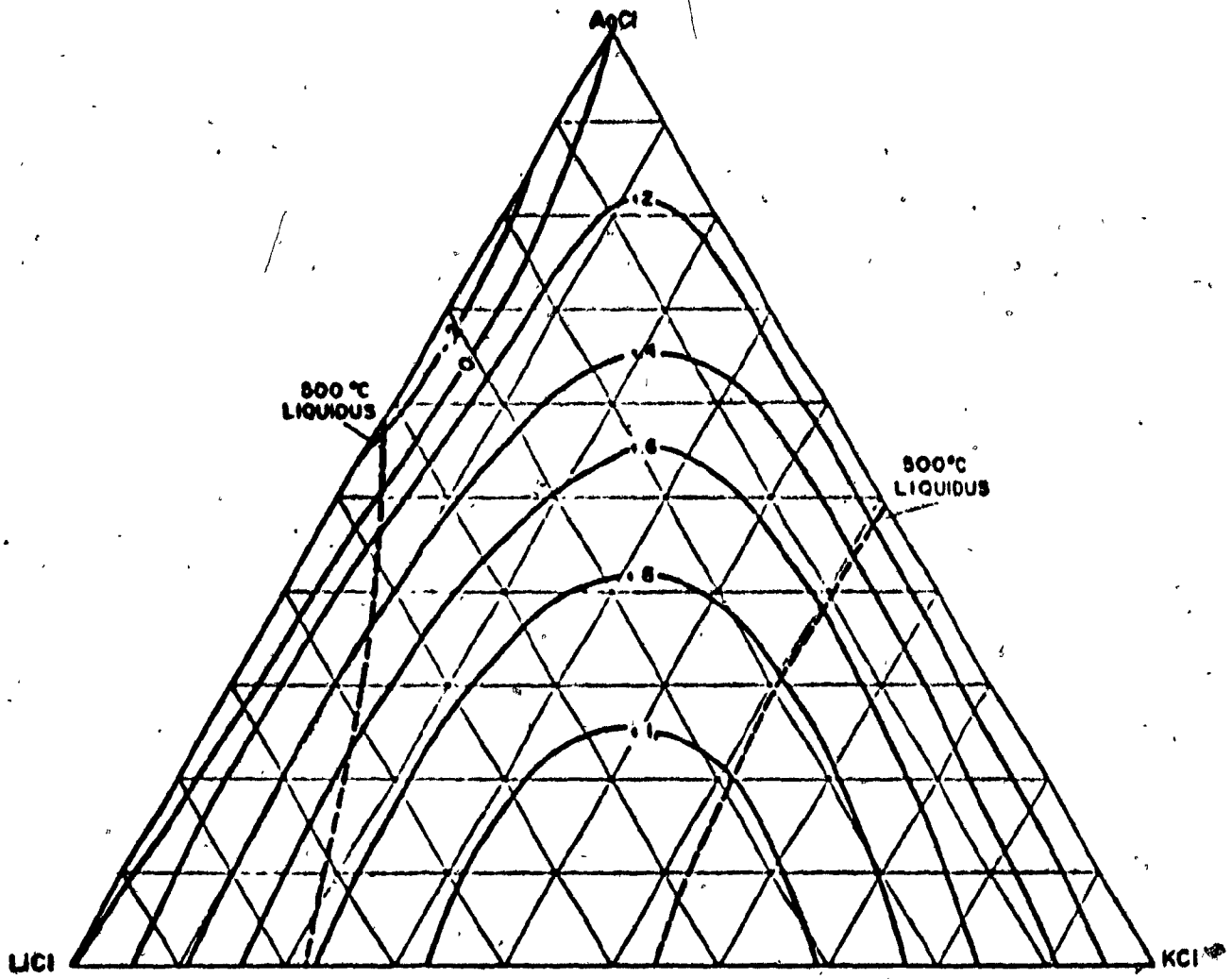

FIGURE 22. ΔS^{E}_{mix} of AgCl-LiCl-KCl.

APPENDIX E

CALCULATED $\Delta\bar{H}$ AND $\Delta\bar{S}$ OF AgCl USING DUAL BONDING MODEL

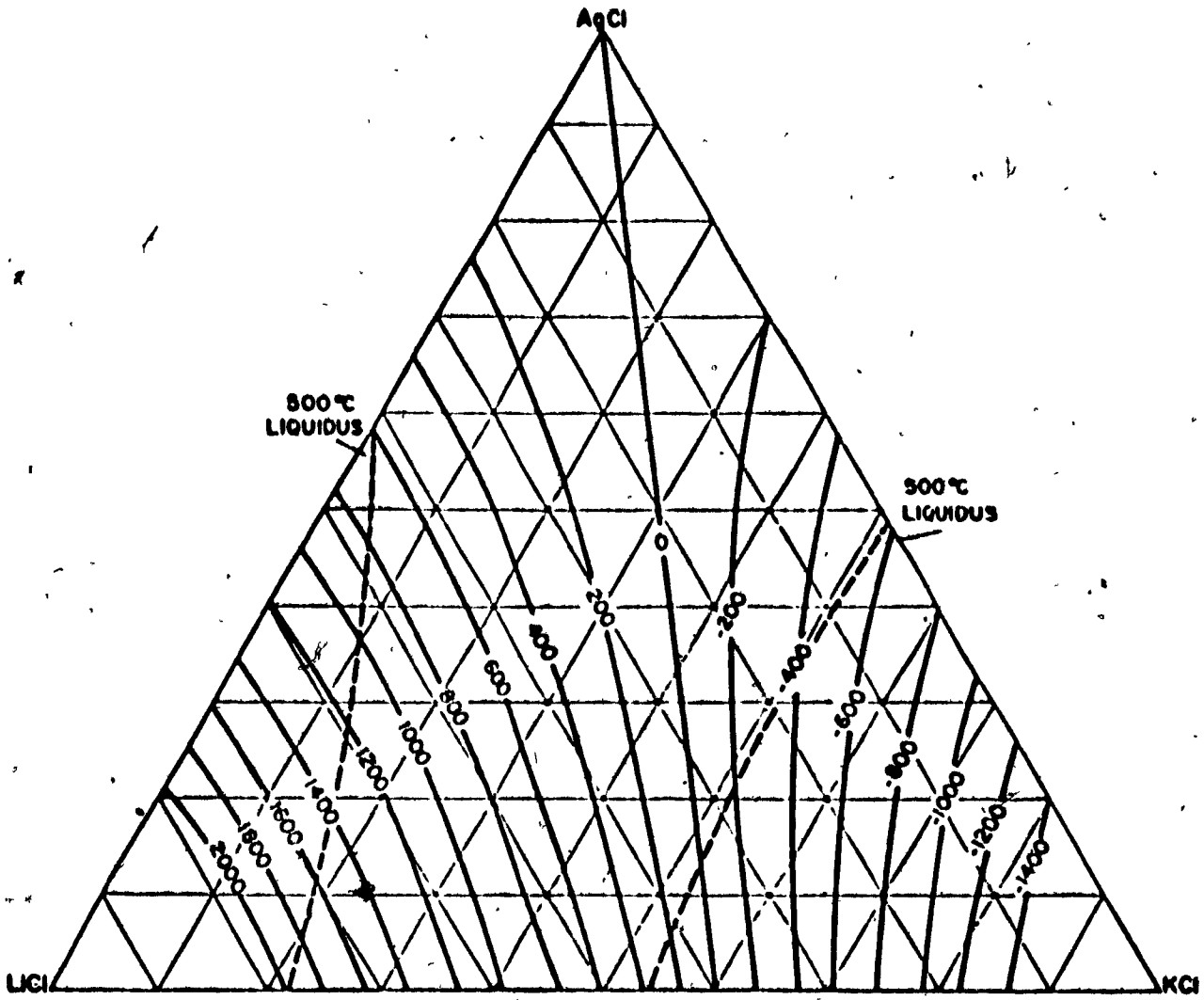

FIGURE 23. $\Delta \bar{H}$ of AgCl as calculated using the dual bonding model. The units are cal./g. mole.

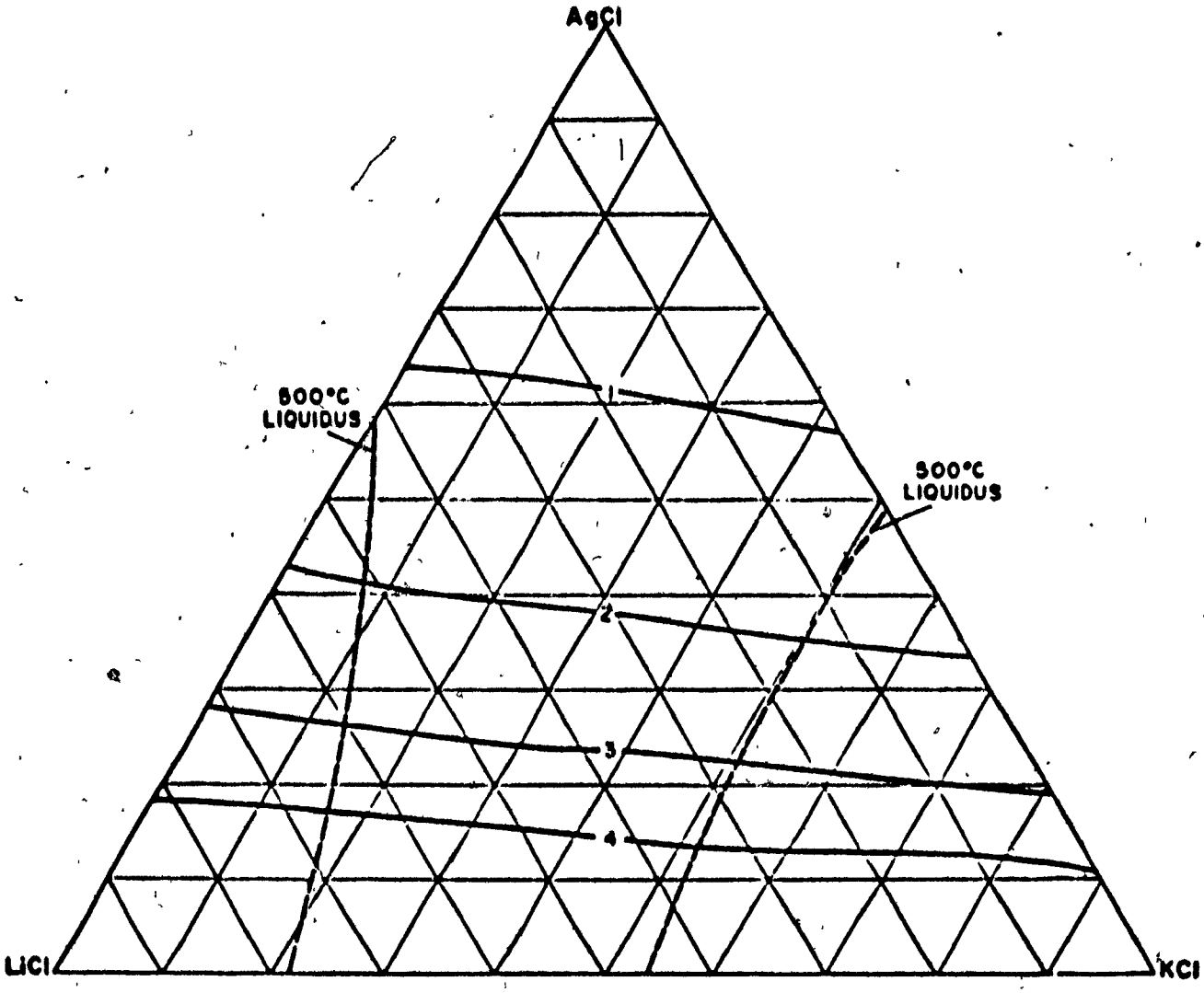

FIGURE 24. $\Delta\bar{S}$ of AgCl as calculated using the dual bonding model. The units are cal./°K g. mole.